

Inconsistent response of Arctic permafrost peatland carbon accumulation to warm climate phases

H. Zhang^{1,2*}, A. V. Gallego-Sala³, M. J. Amesbury^{1,3}, D. J. Charman³, S. R. Piilo^{1,2}, and M. M. Väliranta^{1,2}

¹ECRU, Ecosystems and Environment Research Programme, Faculty of Biological and Environmental Sciences, University of Helsinki, P.O. Box 65, 00014, Finland

²Helsinki Institute of Sustainability Science (HELSUS), Finland.

³Geography, College of Life and Environmental Sciences, University of Exeter, UK.

*Corresponding author: Hui Zhang (hui.palaeo@gmail.com)

Key Points:

- Carbon accumulation in Arctic permafrost peatlands responds inconsistently to warm climate phases
- Recent warming is reflected as increase but also as decrease in carbon accumulation
- Permafrost peatlands are creating a negative feedback to climate warming, but have a probable future scenario to turn to a positive feedback

Abstract

Northern peatlands have accumulated large carbon (C) stocks since the last deglaciation and during past millennia they have acted as important atmospheric C sinks. However, it is still poorly understood how northern peatlands in general and Arctic permafrost peatlands in particular will respond to future climate change. In this study, we present C accumulation reconstructions derived from 14 peat cores from four permafrost peatlands in northeast European Russia and Finnish Lapland. The main focus is on warm climate phases. We used regression analyses to test the importance of different environmental variables such as summer temperature, hydrology and vegetation as drivers for non-autogenic C accumulation. We used modeling approaches to simulate potential decomposition patterns. The data show that our study sites have been persistent mid- to late-Holocene C sinks with an average accumulation rate of 10.80 –

32.40 g C m⁻² y⁻¹. The warmer climate phase during the Holocene Thermal Maximum stimulated faster apparent C accumulation rates (ACARs) while the Medieval Climate Anomaly did not. Moreover, during the Little Ice Age, ACARs were controlled more by other factors than by cold climate per se. Although we could not identify any significant environmental factor that drove C accumulation, our data show that recent warming has increased C accumulation in some permafrost peatland sites. However, the synchronous slight decrease of C accumulation in other sites may be an alternative response of these peatlands to warming in the future. This would lead to a decrease in the C sequestration ability of permafrost peatlands overall.

1 Introduction

Previous peatland studies have suggested that during warm climate phases, e.g., the Holocene Thermal Maximum (HTM, ~ 9000-5000 years ago; Yu et al., 2009) and the Medieval Climate Anomaly (MCA, ~ 950 to 1200 AD; Charman et al., 2013), northern peatland carbon (C) accumulation rates were higher than during cool climate phases. These data originated mainly from boreal peatlands, but comparable data are still scarce at higher latitudes (but see Sannel et al., 2017; Swindles et al., 2015). Thus, the response of Arctic peatlands to, for instance, recent warming (Hartmann et al., 2013) remains uncertain despite the fact that future warming may result in major changes in C accumulation in these high-latitude peatlands. This is partly because warming increases the growing season length and therefore plant productivity, while at the same time plant physiology and decay rates of plant litter are affected by changes in soil moisture conditions. Moisture is an important factor that controls plant net primary productivity (NPP) through impacting photosynthesis (Field et al., 1995). The estimated rate of permafrost loss may be *c.* 4.0 million km² per one degree warming (Chadburn et al., 2017) and permafrost landscapes are likely to get wetter (Oberman, 2008; Romanovsky et al., 2010) or drier (Zhang et al., 2018) in the future depending on microtopographical features. Interlinked changes in temperature and moisture conditions may trigger shifts in vegetation composition (e.g., Zhang et al., 2018) and consequently cause significant changes in C accumulation patterns (Charman et al., 2013; Treat et al., 2016). Moreover, permafrost thaw may expose substantial quantities of old stored organic C to decomposition (Jones et al., 2017; O'Donnell et al., 2012). This could potentially be released to the atmosphere as carbon dioxide (CO₂) and/or methane (CH₄), leading to a positive climate feedback (Hodgkins et al., 2014). The two possible divergent responses of Arctic peatlands: i) an increase in carbon accumulation due to increases in photosynthetic input or ii) an increase in decomposition of plant litter and old carbon due to drying and/or warming, are challenges for C cycle models and future projections (e.g., Schuur et al., 2009). Will predicted

changes in permafrost peatland dynamics lead to a positive or a negative feedback to global warming?

In order to address this question, we selected four permafrost peatlands in northeast European Russia and Finnish Lapland. These regions have experienced increasing temperatures in recent decades (Bekryaev et al., 2010; Bulygina & Razuvaev, 2012; Mikkonen et al., 2015). We investigated changes in C accumulation rates over the past few millennia using a total of 14 peat cores. There was a special focus on warming phases, aiming to provide information for understanding C accumulation responses to future climate warming. Additional local proxy data coming from testate amoeba and plant macrofossil analyses, supplemented by available regional-scale tree ring-based summer temperature reconstructions (Wilson et al., 2016) allowed us to evaluate correlations between C accumulation patterns and various environmental variables.

2 Study sites

The study sites are permafrost peatlands in the discontinuous permafrost zone of Russia and the sporadic permafrost zone in Finnish Lapland (Fig.1 and Table 1). Indico and Seida are located in the Arctic northeast European Russian tundra, where extensive permafrost aggradation occurred from *ca.* 2200 cal. BP onwards (Hugelius, et al., 2012; Routh et al., 2014). During the MCA, permafrost thawing and subsequent desiccation was recorded in our study sites (Zhang et al., 2018). In some parts of our sites, post-Little Ice Age (LIA) warming since 1850 AD has caused permafrost thawing and triggered *Sphagnum* establishment while a stronger recent warming has started to desiccate the peat surface (Zhang et al., 2018). The peat plateaus both at Seida and Indico are elevated a few meters from the surrounding mineral soil, and the vegetation is dominated by shrub-lichen-moss communities, such as *Betula nana*, *Rhododendron tomentosum*, *Empetrum nigrum*, *Polytrichum strictum*, *Sphagnum fuscum*, *S. lindbergii* and sedges of *Eriophorum* spp. In contrast to Seida, peat plateau vegetation at Indico is dominated by lichens and mosses, with less abundant shrubs. On both peat plateaus there are areas of bare peat *c.* 4 meters across (Repo et al., 2009; Ronkainen et al., 2015).

In the Finnish Lapland sites Kevo and Kilpisjärvi, permafrost probably initiated during the LIA around 500-100 cal. BP (Oksanen, 2006; Zhang et al., 2018). Vegetation at both sites is dominated by dwarf shrubs, e.g. *Betula nana*, *Empetrum nigrum*, *Rubus chamaemorus*, *Polytrichum strictum*, *Dicranum* spp, and *Sphagnum* mosses such as *S. fuscum*, *S. balticum*, *S. majus* and *S. riparium* along a hydrological gradient. The sedge *Eriophorum vaginatum* is also present. At Kevo and Kilpisjärvi, there are also patches of bare peat, but they are smaller and less

extensive than those present in the Russian sites.

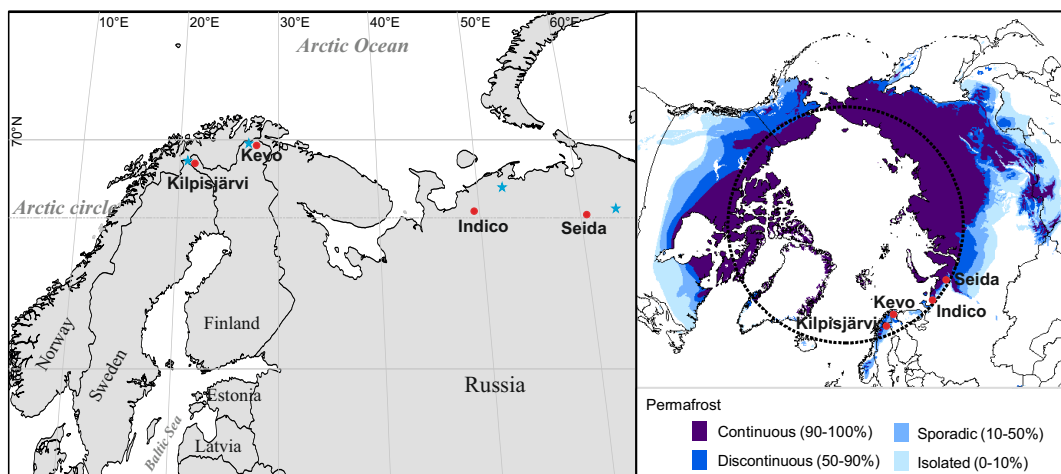


Fig. 1. Location of the study sites (red dots). Climate data for each site are derived from the nearest meteorological station (blue stars), see details in Table 1. Data for circum-Arctic permafrost zonation map are edited from Brown et al. (1998).

3 Materials and methods

3.1 Sampling

In total, 14 active layer peat cores (Table 1) were collected from four sites in August 2012 (Russia) and 2015 (Finland) using a 5 cm diameter Russian peat corer. Individual cores were wrapped in plastic and returned to the lab in sealed PVC tubes and stored in a freezer. The cores were later defrosted and sub-sampled at 1-cm or 2-cm contiguous slices and stored in plastic bags for further analyses.

3.2 Chronology

Due to a lack of preserved and identifiable plant macrofossil remains in our cores, 44 bulk peat samples were sent to the Finnish Museum of Natural History (LUOMUS, Helsinki, Finland) and the Poznan Radiocarbon Laboratory (Poznan, Poland) for accelerator mass spectrometry (AMS) ^{14}C dating (Table 1 and S1). The chronology of the top part of five cores (Table 1) was determined using ^{210}Pb dating. A dry 0.2-0.5 g homogenized subsample from each 1-cm interval was analyzed for ^{210}Pb activity after spiking with a ^{209}Po yield tracer. Details of the applied ^{210}Pb dating method can be found in Ali et al. (2008) and a modified version from the University of

Exeter was used in the laboratory (Estop-Aragonés et al., 2018; Kelly et al., 2017). The surface (0-1 cm) ages of other cores were based on ^{14}C dating, or assumed to be the collecting year. For those cores with surface ages that were assumed to be the collecting year, the first ^{14}C dated depth was always at *ca.* 10 cm (Table 1 and S1).

AMS ^{14}C ages were calibrated using the INTCAL 13 calibration curve (Reimer et al., 2013). Modern dates in pMC (% modern carbon) were converted to radiocarbon ages prior to analysis using the NH Zone1 postbomb curve (Hua et al., 2013). All calibrated mean ages were converted to calendar years before present, where BP is equal to AD 1950. ^{210}Pb ages were obtained through a Constant Rate of Supply model (Appleby & Oldfield, 1978). A preliminary investigation of the R packages Clam and Bacon showed that for several cores Clam (Blaauw, 2010) yielded smaller differences between the modeled age and the dated age when compared to Bacon (Blaauw and Christen, 2011). In addition, Bacon could not be run for core Sei3 BS due to limited amount of dates. Considering the wide application of Clam in peatland studies, the fact that the outputs are highly comparable in the case of high dating density (Blaauw et al., 2018) and our desire to use the same chronological modeling approach for all records, for the current study we chose to use Clam. Age-depth models were developed using Clam (Blaauw, 2010) in R version 3.2.4 (R Core Team, 2014); both ^{210}Pb and ^{14}C dates were included in the model and the smooth spline method was selected initially when developing all age-depth models. Some chronologies yielded age reversals when the default smoothing parameter 0.3 was employed, and if a relatively large deviation of the dated ^{14}C date to age-depth model curve occurred when changing the smoothing parameter, a linear interpolation method was used instead.

3.3 Peat core analysis

3.3.1 Peat properties

Contiguous samples of known volume were extracted from the cores at 1 or 2 cm resolution, oven-dried (50 °C over night and then 110 °C for 6 hours) and weighed to enable calculation of bulk density (g/cm^3). Bulk density was calculated by dividing the dry peat weight by the wet peat volume. Percentage C and N content by mass were measured on homogeneous grounded sub-samples using a LECO TreSpec Elemental Determinator. Carbon-to-nitrogen molar ratios (C/N) were calculated from C and N content measurements. For some cores (Ind1, Ind6, Sei1 and Sei4), loss on ignition (LOI) at 550°C was measured instead of percentage C content (Table S1), for those cores, we assumed that C content was 50% (Loisel et al., 2014).

Table 1. Site and peat core information.

Site	Latitude (N)	Longitude (E)	MAT (°C)	MAP (mm)	GDD0	PAR0	P/Eq	Core	Depth (cm)	Surface age control	Number of ¹⁴ C dates	*Basal age (cal. BP)	MPAR (mm yr ⁻¹)
Indico, Russia	67°16'01"	49°52'59.9"	-4.0	501	1074.27	3649.54	1.57	Ind1	39	Col year	4	3420 ± 64	0.38
								Ind2 BS	38	¹⁴ C	4	7040 ± 48	0.27
								Ind3 BS	48	¹⁴ C	3	6260 ± 24	0.56
								Ind4	35	²¹⁰ Pb	2	2050 ± 65	0.49
								Ind5	45	²¹⁰ Pb	3	7230 ± 64	0.35
								Ind6	44	Col year	3	1885 ± 65	0.31
Seida, Russia	67°07'0.12"	62°57'	-5.6	501	971.65	3165.96	1.63	Sei1	39	Col year	4	6575 ± 88	0.08
								Sei2	24	²¹⁰ Pb	3	3295 ± 82	0.21
								Sei3 BS	30	¹⁴ C	2	6485 ± 85	0.48
								Sei4	29	Col year	2	580 ± 29	0.50
Kevo, Finland	69°49'26.1"	27°10'20.7"	-1.3	433	1151.86	3683.14	1.61	Kev1 BS	31	¹⁴ C	4	1485 ± 72	0.67
								Kev2	33	²¹⁰ Pb	2	1975 ± 78	0.52
Kilpisjärvi, Finland	68°53'4.5"	21°3'11.94"	-1.9	487	985.85	3505.50	1.79	Kil1 BS	40	¹⁴ C	5	3900 ± 73	0.11
								Kil2	32	²¹⁰ Pb	3	1645 ± 78	0.21

Note. Mean annual temperature (MAT) and mean annual precipitation (MAP) data for Indico are from Naryan-Mar meteorological station and cover the period 1961-1990; for Seida are from Vorkuta meteorological station covering the period 1977-2006; for Kevo from Utsjoki Kevo meteorological station and for Kilpisjärvi from Enontekiö Kilpisjärvi Kyläkeskus meteorological station (Pirinen et al., 2012), both for the period 1981-2010. Climate parameters growing-degree days above 0°C (GDD0; temperature sum), cumulative photosynthetically active radiation above 0°C during the growing season (PAR0) and the annual precipitation/annually integrated equilibrium evapotranspiration moisture index (P/Eq) were developed using the CRU 0.5° gridded climatology for 1961-1990 (CRU CL1.0) using PeatStash (Gallego-Sala & Prentice, 2013). BS in core codes represents bare peat surface, other cores are from vegetated surfaces. Ind4 and Ind5 included 10 cm living *Sphagnum* in the top, and Ind5 had mineral mixed bottom part (29-45 cm), those samples were removed for this study. Col year: collecting year. MPAR: mean peat accumulation rate.

3.3.2 Apparent C accumulation rate (ACAR)

Peat vertical growth rates (mm yr^{-1}) were calculated based on the most probable age estimates yielded by the CLAM age-depth model, thus the chronological uncertainties/errors are not taken into account for the further analyses. ACAR ($\text{g C m}^{-2} \text{ yr}^{-1}$) was calculated by multiplying the bulk density of each depth increment by C content and accumulation rate (Tolonen & Turunen, 1996). Both core-specific and site-combined ACARs were calculated. We calculated three different ACAR values: 1) through the whole peat section, 2) between *c.* 1 ka and the coring year and 3) between *c.* 1950 and the coring year.

3.3.3 Peat decay and modeling of past C dynamics

Surface peat is always incompletely decomposed and this needs to be carefully taken into account when comparing recent C accumulation rates with those of the past. To address this challenge we applied the modeling approach developed by Loisel & Yu (2013a) and previously applied, for example, by Wang et al. (2015).

To simulate the potential decomposition processes of the currently only partially decomposed peat, we first identified the boundary between partially and fully decomposed peats (henceforth Dec_{part} and Dec_{full} refer to partially and fully decomposed peats). We used bulk density and C/N value variations (Robinson, 2006; Yu et al., 2001) and the instantaneous rate of change of the age-depth model (Loisel & Yu, 2013a) to determine the as-exact-as possible location of the Dec_{part} and Dec_{full} boundary. In most cores, this boundary approximately occurred in layers dated to *ca.* 100-200 cal. BP. However, occasionally, for example in Kill BS, this boundary corresponded to a shift from deeper *Sphagnum* peat to upper ligneous peat dated to *ca.* 1470 cal. BP. In such cases, we defined the peat formed after AD 1850 as a separate Dec_{part} section to enable the estimation of impacts of recent warming on C accumulation, i.e. the total partially decomposed peat section was divided into two sections but both sections were modeled separately from the Dec_{full} section.

We applied three models (Fig. 2): (1) the exponential decay model (EDM) (Clymo, 1984):

$$M = \frac{p}{\alpha} * (1 - e^{-\alpha*t})$$

where p is the peat addition rate, α is the peat decay coefficient, t is time and M is the observed cumulative peat organic matter pool; (2) the C flux reconstruction model (CFM) (Yu, 2011):

$$\text{NCU}_t = \frac{\text{NCP}_t}{e^{-\alpha * t}}$$

where the net peat C pool (NCP) is used to calculate net C uptake (NCU), α is calculated using EDM, t is time; and (3) a simplified peat decomposition model (PDM) (Frolking et al., 2001):

$$M_t = \frac{p}{1 + \alpha t}$$

where p and α are derived from EDM, M_t is the remaining peat at time t . The EDM, which includes only long-term peat decay processes, was applied to derive p and α using curve-fitting analysis directly from the observed cumulative peat mass data. We applied the EDM separately for the Dec_{part} and Dec_{full} peat sections and assumed that within these sections the peat decay rate was constant (Clymo, 1984). But, if large variations in peat accumulation rates existed inside the sections Dec_{part} or Dec_{full}, we applied the EDM separately to different peat sections to ensure that the most accurate peat decay rate estimates were achieved. These values were then used to drive the CFM (for Dec_{full} peat C fluxes) and the PDM (for Dec_{part} peat C fluxes), which are independent from one another. For Dec_{full} peats, CFM was used to back-calculate the amount of C that was initially deposited (C uptake). For Dec_{part} peats, PDM was used to simulate the potential peat decomposition over a certain period of time and to calculate the remaining amount of peat (which is equivalent to the C uptake if multiplied by the assumed 50% C content in peat organic matter) that will be eventually buried into deeper layers (Loisel & Yu, 2013a).

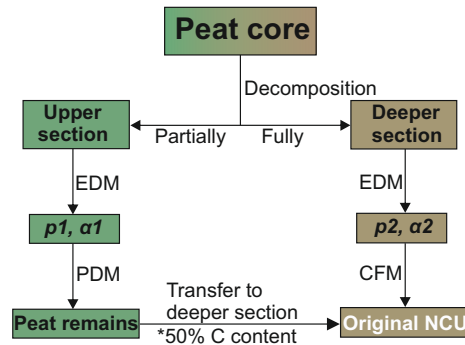


Fig. 2. Flowchart showing the peat decomposition modeling used in this study. Peat cores are divided into upper (partially decomposed) and deeper (fully decomposed) sections according to their decomposition degrees. The exponential decay model (EDM) and peat decomposition model (PDM) are applied to upper sections to estimate the peat remains that will be transferred to deeper sections after simulated future decomposition. EDM and carbon flux reconstruction model (CFM) are applied to deeper sections to back calculate their original net carbon uptake (NCU). 50% of the peat remains from the upper section yield the potential C remains that will be transferred to the deeper section, which is comparable with the calculated original NCU of deeper section. p : peat addition rates; α : peat decay coefficients.

3.3.4 Environmental variables and their links to non-autogenic C accumulation

Testate amoeba or/and plant macrofossil-based water-table depth (WTD) reconstructions were produced at 1-2 cm resolution using the transfer function of Zhang et al. (2017) for testate amoeba and an extended transfer function of Väiliranta et al. (2012) for plant macrofossil data. Vegetation was grouped into three types: herbaceous (grass, forbs, *Equisetum* and Cyperaceae), ligneous (shrubs, trees and rootlets) and bryophytes (mostly *Sphagnum* spp.) according to Treat et al. (2016). In addition to identifiable plant remains, the proportion of unidentifiable organic matter (UOM) was also estimated (see Väiliranta et al., 2007 for the applied method). Tree ring-based last millennium Northern Hemisphere summer temperature (T_{sum}) reconstructions (Wilson et al., 2016) were used to provide a regional climate record, and correspondent T_{sum} for each sample was derived from the published reconstruction curve.

Autogenic processes were considered when studying the effect of environmental variables on C accumulation by fitting decay curve to each profile (Charman et al., 2013). The EDM derived p and α for each core were used to simulate the carbon accumulation rates (CARs) under constant conditions (without external environmental drivers). The differences (ΔCAR) between modeled CARs and actual measured ACARs were considered to be the variation in C accumulation due to non-autogenic (i.e. environmental) processes. Z scores of ΔCAR were then calculated over the total length of cores from each site to enable between-site comparisons.

Correlation analyses of the relationship between non-autogenic ΔCAR z scores and core-specific environmental variables and regional T_{sum} were carried out in R version 3.2.4 (R Core Team, 2014) using the `corr.test` function in the “psych” package to test the relative importance of each variable in determining C accumulation for each core, for each site, for each region and for all cores combined. Only a sub-dataset for the last millennium was used here. Then a multiple linear regression analysis (stepwise) was applied to data from each site, each region and all sites combined dataset to evaluate the influences of variables on overall C accumulation. Three interaction terms ($T_{\text{sum}}*\text{WTD}$, $T_{\text{sum}}*\text{N}\%$ and $T_{\text{sum}}*\text{UOM}$) were used as additional variables.

4 Results

4.1 Chronology and vertical peat accumulation

Vertical peat growth rates were not consistent during the last few millennia (Table 1, S1 and Fig. S1). The depth of the peat cores in our four sites ranged from 24 to 48 cm and the basal ages

ranged from 580 to 7040 cal. BP. The shortest core Sei2 (24 cm) had a basal age of 3295 cal. BP and the age-depth model suggested a hiatus between 1010 to 50 cal. BP. Three cores collected from bare peat surface at Indico (Ind2 BS and Ind3 BS) and Seida (Sei3 BS) gave very old surface ages of 4950, 3660 and 5970 cal. BP respectively (Table S1). These cores were used to investigate long-term C accumulation patterns only and removed from the analysis of peat decay modeling. Two cores collected from bare peat surfaces in Lapland, at Kevo (Kev1 BS) and Kilpisjärvi (Kil1 BS), both yielded modern surface ages (Table S1). Mean peat accumulation rates from all the studied sites ranged from 0.08 to 0.67 mm yr⁻¹ (Table 1). Cores collected from the same site tended to show relatively similar accumulation rates (standard deviation (SD) ≤ 0.10 mm yr⁻¹), but as an exception, Sei3 BS (0.48 mm yr⁻¹) and Sei4 (0.50 mm yr⁻¹) from Seida had clearly higher accumulation rates than Sei2 (0.21 mm yr⁻¹) and especially Sei1 (0.08 mm yr⁻¹). It is notable that at Kilpisjärvi, peat accumulation rates were slower and more stable than elsewhere.

4.2 Peat properties

Peat properties varied with depth and also between different cores and sites (Fig. 4 and Table S1). When data from all the studied cores were combined, the mean bulk density (\pm SD) value was 0.13 ± 0.06 g cm⁻³, which is similar to the mean bulk density (0.111 ± 0.067 g cm⁻³) for peats from western Russia and Fennoscandia (Loisel et al., 2014). N content analyses yielded an average value of $1.49 \pm 0.70\%$, which resembles the value of $1.48 \pm 0.72\%$ reported in a permafrost peat compilation by Treat et al. (2016). The average LOI value was 79.67% with a relatively large SD of 13.86%. The mean C content value of $50.23 \pm 4.37\%$ is slightly higher than the previously reported mean from these regions: $49.2 \pm 3.2\%$ for western Russia and $44.4 \pm 5.7\%$ for Fennoscandia (Loisel et al., 2014), but is still within their standard deviation range. The average C/N ratio was 51.94 with a large SD ± 50.71 . Core specific mean peat property values were variable (Table S1). The average core bulk density ranged from 0.07 ± 0.03 (Ind3 BS) to 0.20 ± 0.05 g cm⁻³ (Sei2). LOI values within cores showed large variations only for core Sei1 with a SD $\pm 18.9\%$, while other measured cores, e.g. Ind6 and Sei4, had more homogeneous LOI values. Additionally, Sei4 had the highest mean LOI value $93.71 \pm 5.70\%$. The measured average core C content of organic matter ranged from 44.92 ± 4.18 (Ind5) to $52.67 \pm 0.79\%$ (Kev1 BS). The average core N content ranged from $0.41 \pm 0.18\%$ (Ind3 BS) to $2.27 \pm 0.22\%$ (Sei3 BS). C/N ratio varied notably between the cores; the range spanned from 23.17 ± 2.27 (Sei3 BS) to 148.61 ± 65.44 (Ind3 BS).

4.3 ACAR variability

Mean long-term ACARs in the Russian sites were $13.66 \text{ g C m}^{-2} \text{ yr}^{-1}$ for Indico and $12.90 \text{ g C m}^{-2} \text{ yr}^{-1}$ for Seida (Table 2). In the Finnish Lapland sites, the Kilpisjärvi cores yielded a lower value of $10.80 \text{ g C m}^{-2} \text{ yr}^{-1}$, while a much higher value ($32.40 \text{ g C m}^{-2} \text{ yr}^{-1}$) was recorded at Kevo (Table 2). Core specific (Fig. 3 and Table 2) ACARs were lowest for Sei1 ($4.32 \text{ g C m}^{-2} \text{ yr}^{-1}$) and highest for Kev1 BS ($33.88 \text{ g C m}^{-2} \text{ yr}^{-1}$). All our cores except the two from Kevo (33.88 and $30.91 \text{ g C m}^{-2} \text{ yr}^{-1}$) had lower ACARs than was reported for northern peatlands ($22.9 \text{ g C m}^{-2} \text{ yr}^{-1}$) in Loisel et al. (2014), but insignificantly ($p = 0.437$) differed from the value reported for permafrost peats ($14.0 \text{ g C m}^{-2} \text{ yr}^{-1}$) by Treat et al. (2016). When the time frame was restricted to the last *ca.* 1 ka (Table 2), cores Ind4 ($29.64 \text{ g C m}^{-2} \text{ yr}^{-1}$), Sei2 ($26.86 \text{ g C m}^{-2} \text{ yr}^{-1}$) and also the two cores from Kevo yielded higher ACARs than $22.9 \text{ g C m}^{-2} \text{ yr}^{-1}$, the mean for northern peatlands (Loisel et al., 2014). When focusing only on recent decades (Table 2), almost all cores had much higher ACARs when compared with the other temporal approaches (entire core and 1 ka), with a largest value of $72.35 \text{ g C m}^{-2} \text{ yr}^{-1}$ for core Kev2. In each case, Indico, Seida and Kilpisjärvi had similar site-based ACARs ($1.2 < \text{SD} < 4.1$), while Kevo had the highest ACAR, approximately twice as high as the other sites.

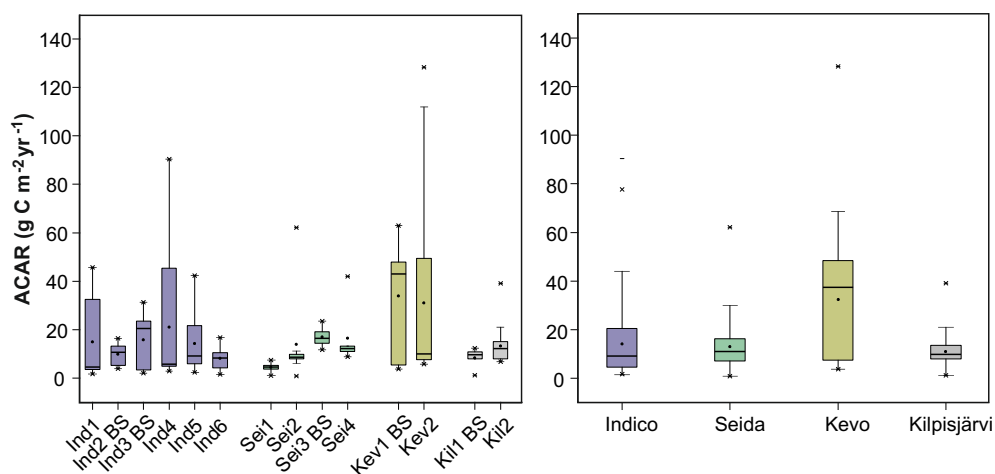


Fig. 3. Apparent carbon accumulation rates (ACARs) for each core (left) and for each site (right). Each color indicates one site. Each box plot shows 1st and 3rd quartiles, median (horizontal lines), mean (dots), and maximum and minimum values (whiskers) and outliers.

For each core, ACARs varied with depth (Fig. 4). The very high ACARs reported from, for example, core Ind1 ($38.25 \text{ g C m}^{-2} \text{ yr}^{-1}$) and Kev1 BS ($42.71 \text{ g C m}^{-2} \text{ yr}^{-1}$) around 1500 cal. BP were unrealistically high and may have resulted from chronological uncertainties (see also Sannel et al., 2017). In order to evaluate the temporal patterns of ACARs for each site, we

grouped ACAR data into 100-year bins for the last 1000 years and 200-year bins before that (Fig. 5). The above-mentioned conspicuously high values (Fig. 5a-d) were omitted from further data analysis. A combined ACAR history from which the high ACAR peaks and also the recent incompletely decomposed peats had been removed is shown in Fig. 5e. At Indico (Fig. 5a), a high ACAR phase ($15\text{-}20 \text{ g C m}^{-2} \text{ yr}^{-1}$) was dated to around 7000-6000 cal. BP, after this the ACARs declined to $5\text{-}10 \text{ g C m}^{-2} \text{ yr}^{-1}$. During the last millennium, ACARs gradually increased, with some fluctuations until a sharp increase started at 100-0 cal. BP. At Seida (Fig. 5b), a similar high ACAR phase was detected and dated to 6000-7000 cal. BP and to recent decades. At Kevo (Fig. 5c) stable and low ACARs persisted until a significant increase started *ca.* 100-0 cal. BP. At Kilpisjärvi (Fig. 5d) a gradual increase in ACAR started *ca.* 1800 cal. BP but there has been a more pronounced increase in ACAR during the recent years. When all sites and data were combined (Fig. 5e), highest ACARs (*ca.* $15 \text{ g C m}^{-2} \text{ yr}^{-1}$) occurred during 7000-6000 cal. BP then decreased sharply to *ca.* $5 \text{ g C m}^{-2} \text{ yr}^{-1}$. Subsequently, a gradual increase in ACAR ended with a minor peak ($12 \text{ g C m}^{-2} \text{ yr}^{-1}$) at around 350 cal. BP.

4.4 Peat decay and modeling of C dynamics

The exponential decay model (EDM) yielded various decay coefficients and peat addition rates for different peat sections of the studied 11 cores (Table S2). Generally, and as expected, higher decay coefficients (α) were derived for Dec_{part} peats, though the values varied a lot. For Dec_{part} layers, the largest value was $117.70 \times 10^{-4} \text{ yr}^{-1}$ (Ind4) and the lowest value was $4.11 \times 10^{-4} \text{ yr}^{-1}$ (Ind6). For the Dec_{full} peat sections, the largest value was $9.57 \times 10^{-4} \text{ yr}^{-1}$ (Ind5) and the lowest value was $0.18 \times 10^{-4} \text{ yr}^{-1}$ (Kev2). Peat addition rates (p) confirmed the pattern where Dec_{part} peats had higher accumulation rates than Dec_{full} layers.

The C flux reconstruction model (CFM) suggested net C uptake ($\text{g m}^{-2} \text{ yr}^{-1}$, NCU) for the Dec_{full} peat sections (Table S3), ranging from 4.04 to $13.77 \text{ g m}^{-2} \text{ yr}^{-1}$. These estimates represented the average annual peat C flux that entered the Dec_{full} sections over the past few millennia. The peat decomposition model (PDM) simulated the remaining peat C mass of the Dec_{part} layers after 100 (ranged from 1.32 to $50.36 \text{ g m}^{-2} \text{ yr}^{-1}$) and 300 years (ranged from 1.20 to $34.61 \text{ g m}^{-2} \text{ yr}^{-1}$) of decomposition. After a decomposition simulation of 100 years, eight out of eleven cores yielded higher remaining peat C mass ($\text{g m}^{-2} \text{ yr}^{-1}$) than the average value of the modeled past NCU, i.e. more NCU was derived for the Dec_{part} peats than Dec_{full} peats, while only seven of them continued to yield the same result when the setting decomposition time was changed to 300 years (Fig. 6).

Table 2. Apparent carbon accumulation rates (ACARs) ($\text{g C m}^{-2} \text{yr}^{-1}$) since basal, 1 ka and recent past of peat cores from the four studied permafrost peatlands.

		Since basal		Since ca.1 ka (950 AD)				Since recent years (after 1950 AD)			
		ACAR	Average ACAR/site	Depth (cm)	Age (cal. BP)	ACAR	Average ACAR/site	Depth (cm)	Age (cal. BP)	ACAR	Average ACAR/site
Indico	Ind1	14.93		11	1125	6.24		2	-4	11.52	
	Ind2 BS	9.74		-	-	-		-	-	-	
	Ind3 BS	15.54		-	-	-		-	-	-	
	Ind4	20.99		27	1020	29.64		19	-3	56.99	
	Ind5	12.59		27	1115	13.22		11	3	41.23	
	Ind6	8.14	13.66	33	1062	8.96	14.52	3	-4	10.51	30.06
Seida	Sei1	4.32		10	1061	2.92		1	-24	4.76	
	Sei2	13.92		7	1012	26.86		5	-3	36.22	
	Sei3 BS	16.89		-	-	-		-	-	-	
	Sei4	16.48	12.90	29	600	16.48	15.42	5	-15	36.42	25.80
Kevo	Kev1 BS	33.88		24	989	34.44		6	-8	43.70	
	Kev2	30.91	32.40	26	1083	36.95	35.70	7	-11	72.35	58.03
Kilpisjärvi	Kil1 BS	8.35		15	1013	10.59		1	-56	8.42	
	Kil2	13.24	10.80	24	1005	15.00	12.80	3	-10	31.70	20.06

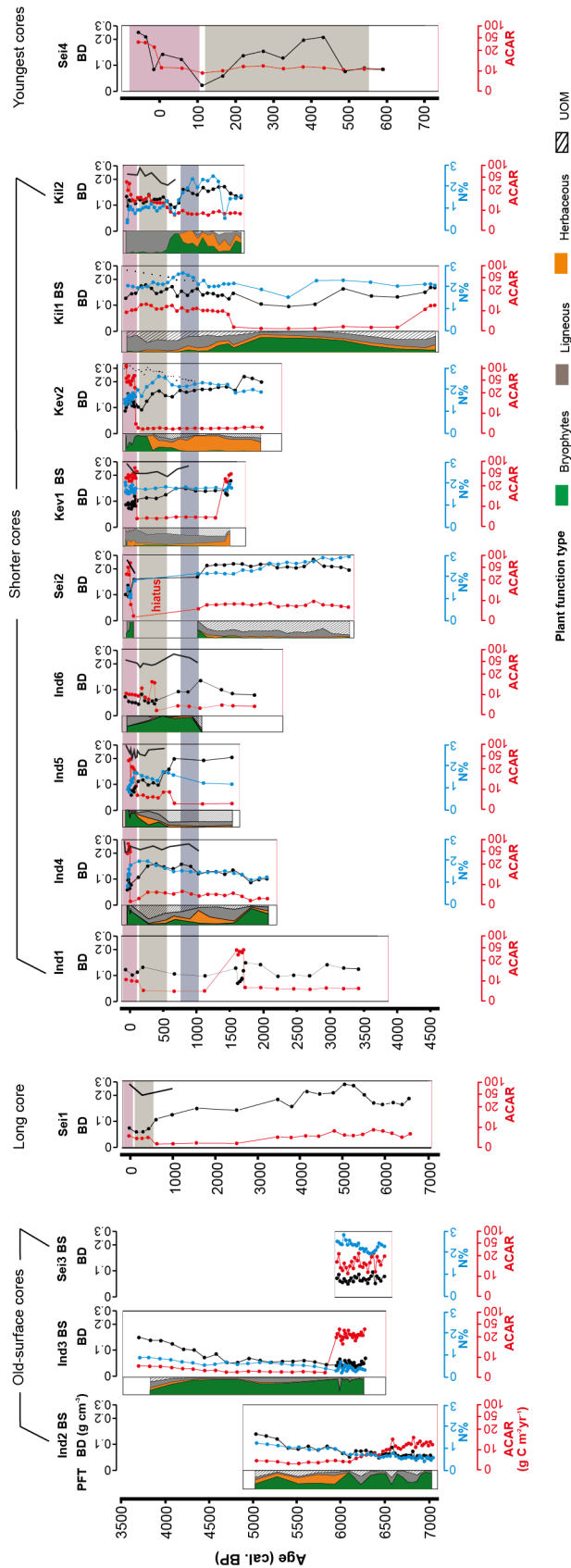


Fig. 4. Bulk density (BD), nitrogen content (N%) and apparent carbon accumulation rates (ACARs) plotted against age for the studied cores. Plant macrofossil results of analysed 10 cores are shown using plant function types (PFT). Black lines (without symbols) indicate hydrological shifts reconstructed using testate amoeba data, and black dash lines indicate results from plant macrofossil data (left: wet; right: dry; no scales are shown). Note four sets of Y-axes (ages) are used. Climate phases are indicated using purple (Medieval Climate Anomaly), gray (Little Ice Age) and red (recent warming) shadings.

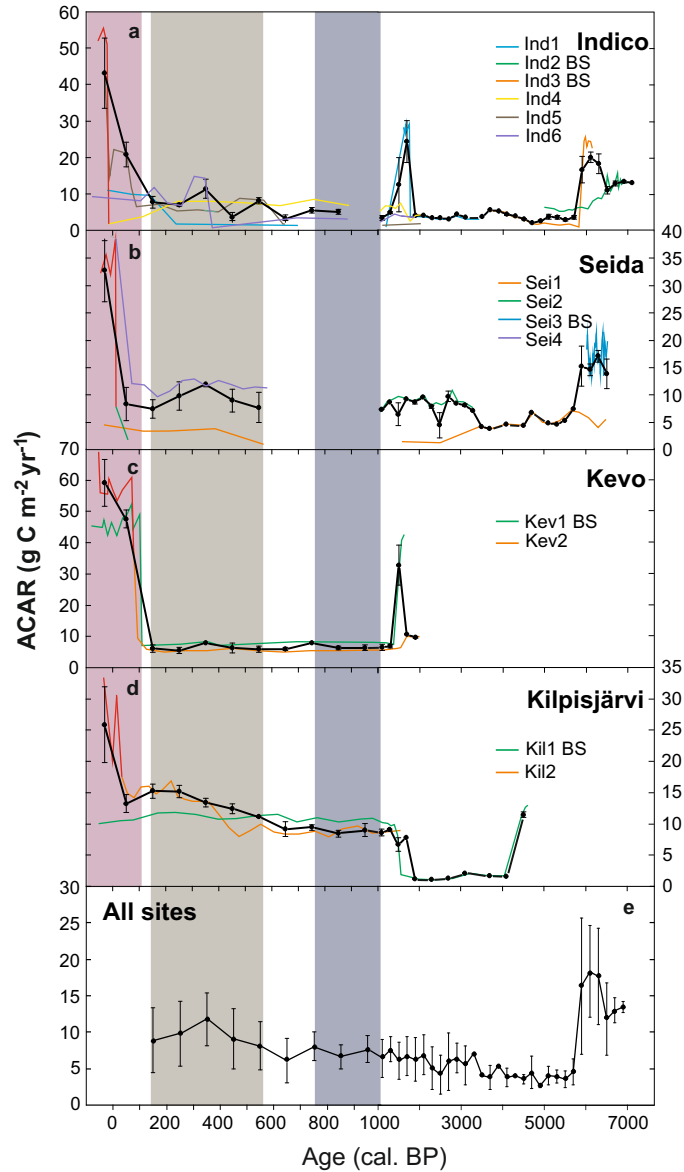


Fig. 5. (a-d) Apparent carbon accumulation rates (ACARs) for four permafrost peatlands with error bars representing standard errors of the means (standard deviation of its sampling distribution to the means). Up to 1000 yrs BP, calculations are for each 100-yr bin, for the later periods, calculations are for each 200-yr bin. (e) Combined data for all sites after removing those samples that may be influenced by uncertainty of ^{14}C dating and samples accumulated since 100 cal. BP (see text for details). In each site, ACARs presented by the red curve in recent warming period is rescaled (see Fig. 4 for original values). Climate phases are indicated using purple (Medieval Climate Anomaly), grey (Little Ice Age) and red (recent warming) shadings.

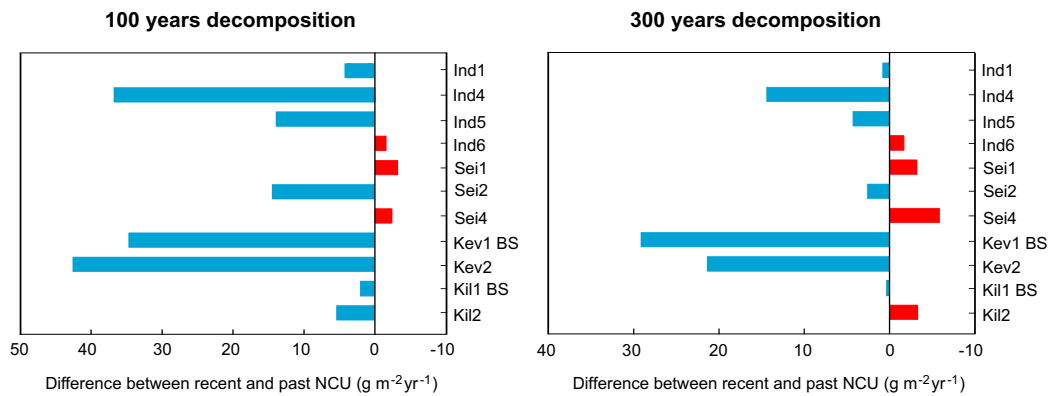


Fig. 6. Differences between the expected remaining C mass of recent accumulated peat after 100 and 300 years decomposition and the original net peat C uptake (NCU) during the past few millennia (from *c.* 100 cal. BP to the bottom age of the cores). Blue bars indicate that recent NCU is higher than that of the past, and red bars indicate the opposite pattern.

4.5 Non-autogenic C accumulation and correlations with environmental variables and regional summer temperature

Non-autogenic CAR z scores were grouped into 100-year bins for the last 1000 years and 200-year bins before that (Fig. S2). At Indico, C accumulation for different cores showed fluctuations around 7000-6000 cal. BP. From 6000 to 2000 cal. BP, C accumulation was stable. After that, C accumulation for individual cores showed large fluctuations especially during the LIA and the recent warming period. Overall, C accumulation was faster during the LIA than any other period. At Seida, higher C accumulation phases were dated to 6000-4000 cal. BP, the LIA and post 1950 AD. During the recent warming period, different cores showed large variations. At Kevo, overall stable C accumulation has persisted until present. Before 100 cal. BP, different cores showed small variation, while after 100 cal. BP very large variations were detected. At Kilpisjärvi, reduced C accumulation occurred around 2000, 650 and 50 cal. BP. Two cores showed large variations for the transition period from the MCA to LIA, and post 1950 AD. When data from all sites were combined, increased C accumulation occurred before *ca.* 3000 cal. BP, then C accumulation declined until the LIA. A distinct increase of C accumulation happened during the LIA. During recent warming, first a decline happened which was followed by a latter increase in C accumulation.

Correlation analyses showed that only in a few cases there was a relationship between non-autogenic CAR z scores and the studied environmental variables (Table 3). Core Sei2 showed a strong significant positive correlation ($r = 0.97$, $p < 0.05$) between WTD and non-

autogenic CAR z scores. Kev1 BS yielded significant correlations between N content ($r = 0.42$, $p < 0.05$), C/N ($r = -0.42$, $p < 0.05$), WTD ($r = 0.60$, $p < 0.05$) and non-autogenic CAR z scores. The rest of the cores suggest that there are no correlations. The analysis of combined data showed a significant weak negative correlation to bryophytes proportion ($r = -0.23$, $p < 0.05$), while no correlations were observed for other variables. Non-significant relationships between individual variables and non-autogenic CAR z scores suggest that the relationships are non-linear, multivariate or some of the drivers have not been identified. The multiple linear regression analysis for Seida site yielded a model (adj. $R^2 = 0.91$, $p = 0.03$) with only WTD as the significant variable, while the analysis for all sites combined dataset yielded a poor model (adj. $R^2 = 0.04$, $p = 0.04$), including only bryophyte proportion as the significant variable. But beyond that, the multiple linear regression analyses for other sites and two regions ended up with no valid variables (stepwise method).

Table 3. Correlation coefficients (r) between non-autogenic carbon accumulation rate z scores and environmental variables for each core, each site, each region and all sites combined.

	T _{sum}	N%	C/N	WTD	Bry	Her	Lig	UOM
Ind4	-0.01	-0.23	0.40	-0.04	-0.06	0.11	-0.13	0.16
Ind5	0.47	-0.06	0.23	0.18	-0.26	0.30	0.15	0.16
Ind6	-0.27	-	-	-0.51	-	-	-	-
Indico	0.02	-0.14	0.32	-0.02	-0.15	0.16	0.01	0.16
Sei1	0.34	-	-	0.10	-	-	-	-
Sei2	0.13	-0.29	0.38	0.97 *	-0.73	0.01	0.73	-0.03
Seida	-0.01	-0.29	0.38	0.46	-0.73	0.01	0.73	-0.03
NEE Russia	-0.01	-0.19	0.25	0.14	-0.45	0.09	0.45	0.09
Kev1 BS	0.13	0.42 *	-0.42 *	0.60 *	0.19	-0.15	0.04	-0.05
Kev2	0.16	0.02	0.04	0.09	-0.20	-0.02	0.25	-0.03
Kevo	0.13	0.05	0.01	0.11	-0.15	-0.02	0.22	-0.03
Kil1 BS	-0.21	-0.05	0.11	-0.12	-0.04	0.29	-0.46	0.31
Kil2	0.11	0.04	-0.01	0.45	-0.25	0.05	0.45	-0.03
Kilpisjärvi	0.06	0.08	-0.03	0.18	-0.25	0.06	0.13	0.05
Lapland	0.11	0.05	0.00	0.12	-0.17	0.02	0.13	0.02
All sites	0.06	-0.03	0.11	0.11	-0.23*	0.03	0.19	0.04

Note. Significant correlations are given (* $p < 0.05$). Tsum: summer temperature. Bry: Bryophytes. Her: Herbaceous. Lig: Ligneous.

5 Discussion

When predicting the fate of permafrost peatland C sequestration and storage under future climate warming, it is useful to understand past relationships between climate and peatland dynamics. The drivers of C sequestration are complex, and several processes need to be considered. For instance, it has been suggested that warming could result in the transformation of permafrost peatlands to fen environments. This would promote high ACARs due to increased productivity because of warming and reduced decomposition in moisture saturated, anoxic peat, although even if this is the case, the net radiative effect remains uncertain because of the potential increase of methane emissions (Swindles et al., 2015). Moreover, studies on high-latitude non-permafrost peatlands suggest that there will be a warming-induced vegetation change from minerotrophic fen conditions to more oligo- and ombrotrophic *Sphagnum*-dominated conditions that may enhance the C sink capacity of peatlands (Loisel & Yu, 2013a), or unchanged vegetation but with increased NPP stimulated by warmer temperatures and longer growing seasons (Klein et al., 2013a). This might be potentially one trajectory for permafrost peatlands. Additionally, only small immediate changes in NPP may occur linked to permafrost thaw due to tradeoffs between slow growth rates of long-lived woody plants on dry surfaces and more responsive bryophyte community growth in collapsed wet depressions (Camill et al., 2001). There is also evidence that warmer temperatures and wetter conditions enhance C sequestration and thus peat accumulation, i.e. increase the net peatland C uptake (Wilson et al., 2017).

The environmental data for the last millennium that we achieved in this study show core-specific variability (Fig. 4). But we also recorded some comparable features to previous studies. For example, in Russia the MCA warming resulted in permafrost thawing and the consequent establishment of moist fen-type communities (Ind4) (Zhang et al., 2018), which correspond to previous European Russian studies (e.g., Routh et al., 2014). However, these moist communities were subsequently replaced by shrubs and dry conditions, which were supported by testate amoeba reconstructions. A dry MCA has been reported from a nearby region (Kremenetski et al., 2004) and some other areas for example in Arctic Canada and southern Finland (Helama et al., 2009). During the LIA, Finnish sites appear to have been wet at the beginning of the LIA, which corresponds to the humid climate recorded in Finland (Linderholm et al., 2018; Väliiranta et al., 2007). Both Russian and Finnish sites suggest habitat changes towards drier communities over recent decades. A similar trend was also found previously in northern Sweden (Gałka et al., 2017). Chronologically, this habitat change corresponds to extensive permafrost degradation reported for the last c. 50 years (Jones et al., 2016; Kokfelt et al., 2009). A multiple linear regression between these environmental variables and ACAR data suggest that summer

temperature ($\beta = 22.53$, $p = 0.002$), WTD ($\beta = 6.28$, $p = 0.018$) and UOM ($\beta = -0.40$, $p = 0.017$) are significant explanatory variables explaining overall ACAR patterns (Table S4). A previous study indicated that under warmer temperatures apparent recent carbon accumulation is higher in wet microhabitats than in dry habitats, due to lower decomposition rate (McLaughlin & Webster, 2014). In the current study plant functional types were not significant variables, which is in contrast to the pattern found for southern peatlands (Loisel & Yu, 2013b). However, all the detected significant variables in our data are linked to decomposition, which indicates the possible influence of autogenic processes, namely long-term decay, on the relationship. After removing the autogenic trend, none of our studied environmental variables were consistently highlighted as significant drivers on C accumulation (Table 3). This suggests that the response of permafrost peatland carbon accumulation dynamics to climate is more complex than expected, and there may be interactions between permafrost and the possible environmental variables, which may respond differently depending on local conditions. To date the autogenic peat decay models do not include the permafrost dynamics-induced peat decay changes that largely influence carbon dynamics (see Jones et al., 2017; O'Donnell et al., 2012). Therefore, future efforts in understanding the links between permafrost dynamics and decay changes are required to more accurately investigate the relationships between carbon accumulation and environmental variables.

5.1 Local-scale inconsistencies in carbon accumulation patterns

Replicated records from the same peatland should provide a more robust picture of past peatland dynamics (Loisel & Garneau, 2010; Mathijssen et al., 2016, 2017; Pelletier et al., 2017; Zhang et al., 2018). Our study supports the need for replication. We detected relatively large internal ACAR variations at most of the peatland sites (Fig. 3-5 and Table 2). For example, at Indico the mean ACAR for each core ranged from 8.14 to 20.99 g C m⁻² yr⁻¹ and at Seida from 4.32 to 16.89 g C m⁻² yr⁻¹. Our data include only three records (Ind2 BS, Ind3 BS and Sei3 BS) with old basal ages > 6000 cal. BP, meaning that only these captured part of the HTM (Holocene Thermal Maximum) when peat accumulation was presumably higher than during the late Holocene (Loisel et al., 2014; Yu et al., 2010). In general, our records represent a shorter period of time and accordingly the mean ACAR values are lower than for those reported earlier from similar regions (Botch et al., 1995; Oksanen, 2006; Oksanen et al., 2003; Turunen, 2003).

External environmental factors sometimes had opposite influences on carbon accumulation rates in different cores (Fig. S2). For instance, during the LIA core Ind6 suggested

a large increase while other cores showed stable or slightly decreased rates; during the transition from the MCA to LIA, two cores from Kilpisjärvi also experienced adverse pattern. Such a pattern where C accumulation of adjacent cores, a few meters apart, respond differently to the same external driver was also reported by Gao & Couwenberg (2015). Even in those cases when external drivers had the same forcing, either leading to increase or decrease in C accumulation, respectively, the magnitudes varied.

Permafrost aggradation probably explains some of the very low ACAR values $<5 \text{ g C m}^{-2} \text{ yr}^{-1}$ detected in, for example, Ind1 *ca.* 3500-2200 cal. BP, Sei1 *ca.* 3495-580 cal. BP and Kev1 BS *ca.* 1445-140 cal. BP (Fig. 4) (Bauer & Vitt, 2011; Garneau et al., 2014; Hunt et al., 2013; Seppälä, 2006). During these periods peat accumulation rates were as low as $2 \times 10^{-5} \text{ m}^{-2} \text{ yr}^{-1}$. Moreover, a long-term hiatus in the accumulation record may occur, as has been detected in the age-depth model of Sei2 (see also Routh et al., 2014 and Sannel et al., 2017). In addition, the very low carbon accumulation rates, when followed by thaw, could also be the results of peat decomposition of the formerly frozen peat layers upon thaw (see Jones et al., 2017; O'Donnell et al., 2012). In contrast, permafrost thaw may have resulted in also very high ACARs ($> 50 \text{ g C m}^{-2} \text{ yr}^{-1}$) as recorded in Ind4 and 5, where *Sphagnum* is encouraged to grow in-situ by the hydrological changes brought about by warming (Zhang et al., 2018).

5.2 Regional-scale inconsistencies in carbon accumulation patterns

In addition to small-scale habitat factors driven by microtopography, ACAR patterns can be expected to vary between different climate regimes (Charman et al., 2015). In general, the ACAR values detected in this study $\sim 12 \text{ g C m}^{-2} \text{ yr}^{-1}$, are notably low when compared with the average of $22.9 \text{ g C m}^{-2} \text{ yr}^{-1}$ for northern non-permafrost peatlands (Loisel et al., 2014), probably due to the smaller Arctic net primary production and standing biomass (Saugier et al., 2001).

Spatial variation in NPP is driven by growing-degree days above 0°C (GDD0) and cumulative photosynthetically active radiation above 0°C during the growing season (PAR0) at hemispheric scales (Charman et al., 2013). Between our study sites there are no large variations in these indices, but at Kevo GDD0 and PAR0 are slightly higher than at the other sites (Table 1). This may partly explain recorded high ACARs at Kevo, in addition to the influences of incomplete decomposition. Correlation analysis between mean ACARs for each core and climate parameters, that is the same for each site, showed that GDD0 was significantly correlated to ACARs ($r = 0.651$, $p = 0.012$). This is in line with studies published for some boreal and

subarctic peatlands (Garneau et al., 2014), while PAR0 and the moisture index P/Eq yielded no significant correlations, although the number of sample sites is small and the range in GDD0 and PAR0 is also limited. This is in contrast with previous suggestions that PAR0 explains variations in C accumulation more strongly than GDD0 (Charman et al., 2013; Xing et al., 2015). Growing season warmth expressed as temperature sum (GDD0) could influence both NPP and decomposition, while PAR0 is an important control on NPP, thus our data may highlight the importance of decomposition on Arctic permafrost peatland C accumulation process. Nevertheless, the positive correlation between GDD0 and ACARs suggests that NPP must have been increasing more than decomposition under a warming climate. In this study we did not find a significant relationship between ACARs and the moisture index P/Eq. However, this does not preclude the importance of moisture on ACARs when associated to local-scale permafrost peatland dynamics (Gałka et al., 2017; Swindles et al., 2015; Zhang et al., 2018).

5.3 Response of C accumulation to warmer climate phases

5.3.1 Response to historical warm climate

The distinct higher ACARs around 7000-6000 cal. BP correspond to the suggested Holocene-scale pattern for northern peatlands (Loisel et al., 2014; Yu et al., 2010). In contrast to the HTM, warm MCA did not trigger rapid C accumulation development (Fig. 4 and 5). One important difference between these two warm phases is that, at least in Russia, the MCA was preceded by permafrost-occupied conditions, while there was no permafrost before or during the HTM. This is in line with previous studies where no link between warm summers and C accumulation patterns on permafrost peatlands was found (Gao & Couwenberg, 2015). The MCA was also a considerably shorter period than HTM and the spatial features, geographic distribution and strength of the anomaly were more variable (Mann, 2002). Thus, the MCA signature may be less clearly detectable in our sites (Zhang et al., 2018).

Interestingly our data did not indicate an overall decline of C accumulation from the MCA to LIA that was visible for more southern bog peatlands (Charman et al. 2013), instead distinct higher C accumulation occurred during the LIA. Similarly, Gao & Couwenberg (2015) reported of carbon accumulation peaks which occurred during the Little Ice Age. Therefore, in sub-Arctic regions, during cold periods, ACAR dynamics may be controlled more by hydrology-related decomposition processes rather than by low productivity (Klein et al., 2013b).

5.3.2 Response to recent warming

The ACARs were typically much higher for the upper peat sections which accumulated after 200-100 cal. BP (e.g., Lamarre et al., 2012; Loisel et al., 2010), obviously partly because complete decomposition of plant material has not yet occurred. After taking into account potential decomposition processes using three different approaches, the results from those upper peat sections yielded comparable rates to those calculated from the past one to seven millennia (Fig. 6).

For most of the peat sections, after 100 and 300 years of decomposition, respectively, the CAR will still be greater than that of the past few millennia (Fig. 6), suggesting an increased C sink capacity. Longer and warmer growing seasons during the recent decades may have played a key role in the observed increase in CAR through stimulated NPP (Charman et al., 2013). In addition, changes in vegetation (Loisel & Yu 2013a; Treat et al., 2014) from sedges to Sphagna, and possibly decrease in N% probably indicating decrease in decay rates (Bragazza et al., 2012; Charman et al., 2015; Sannel & Kuhry, 2009), seem to explain part of the enhanced C sink capacity (Fig. 4).

For some of the records, the simulated decomposition models predicted lower CAR than that calculated for the preceding millennia (Fig. 6). For these sites the supposedly positive effect of higher temperature and increased solar radiation cannot counterbalance the negative effect caused by, for instance, moisture deficiency (Zhang et al., 2018). Consequently, similar to some boreal peatlands (e.g., Nichols et al., 2014), it is possible that these sites are transforming into environments which sequester atmospheric C less efficiently, and thus create a positive accelerating feedback for anthropogenic warming.

These inconsistent responses of Arctic permafrost peatland C dynamics to past warming phases and to recent warming indicate that sensitivity of these ecosystems to warming is not straightforward (see also Gao & Couwenberg, 2014). This complicates understanding their future role in global biogeochemical cycles under the warming climate. Under warm conditions, C accumulation may increase due to higher NPP, while it may also decrease because of increased evapotranspiration or drainage processes which cause moisture deficiency (e.g., van Bellen et al., 2011). In addition, warming may stimulate decomposition, but in turn severe water deficiency may limit microbial activity (Faucherre et al., 2018). The final C uptake ability is also linked to, for instance, local microtopographical conditions. Intense permafrost thawing eventually causes

peatland collapse and saturation with thaw water potentially leading to increase in carbon sequestration through increased NPP and decreased CO₂ emissions, although wetting promotes CH₄ emissions (Swindles et al., 2015). Also some studies suggest that critical loss of sporadic and discontinuous permafrost in the coming century may lead to a loss of the large deep C storage (Jones et al., 2017; Schuur et al., 2015). Thereby in the future the net effect can either be an increase or a reduction in ACARs, or even turning the site to a net C source (Chaudhary et al., 2017; Wang et al., 2015; Zhang et al., 2013).

6. Conclusions

Sub-Arctic peatland data from northeast European Russia and Finnish Lapland indicated complex carbon (C) accumulation patterns during the past few millennia. Large variations in C accumulation rates occurred both at the local and regional scales. A range of possible environmental drivers were investigated but no consistent relationship with temporal variations in carbon accumulation rates were detected. However, permafrost aggradation and thawing were important factors influencing C accumulation.

Warm climate phases seems to have triggered increase in C accumulation during the Holocene Thermal Maximum and recent decades, but the same pattern did not occur during the Medieval Climate Anomaly. Moreover, the response of C accumulation rate to recent warming was not consistent, as both increased and decreased C accumulation patterns were detected. The Little Ice Age had a weak forcing on C accumulation as the data indicated relatively high C accumulation rates for that period. Future C dynamics might depend not only on the magnitude of temperature increase per se and associated decomposition changes, but also on local-scale permafrost dynamics and consequent changes in hydrology and vegetation. A cautious conclusion is that permafrost peatlands may create a short-term negative, cooling, feedback to climate warming, but that there is a probable risk they turn to positive feedback elements in the future.

Acknowledgements

HZ acknowledges the financial support of the China Scholarship Council for her PhD study (grant no. 201404910499) at the University of Helsinki. The research presented in this article was financed by the Academy of Finland and University of Helsinki. The work done by DJC and

AGS was funded by the Natural Environment Research Council (NERC standard grant number NE/I012915/1) and supported by NERC Radiocarbon Allocation 1681.1012. We thank Dr. Weiyu Zhang for help with mathematical calculations, Pirita Oksanen and Paul Mathijssen for assisting with fieldwork. We thank the reviewers and editors for their constructive comments. The data used in this study are included in the tables, figures and supplements, or are available in the cited references.

References

- Ali, A. A., Ghaleb, B., Garneau, M., Asnong, H., & Loisel, J. (2008). Recent peat accumulation rates in minerotrophic peatlands of the Bay James region, Eastern Canada, inferred by ^{210}Pb and ^{137}Cs radiometric techniques. *Applied Radiation and Isotopes*, *66*, 1350-1358.
<https://doi.org/10.1016/j.apradiso.2008.02.091>
- Appleby, P. G., & Oldfield, F. (1978). The calculation of ^{210}Pb dates assuming a constant rate of supply of unsupported ^{210}Pb to the sediment. *Catena*, *5*, 1-8.
[https://doi.org/10.1016/S0341-8162\(78\)80002-2](https://doi.org/10.1016/S0341-8162(78)80002-2)
- Bauer, I. E., & Vitt, D. H. (2011). Peatland dynamics in a complex landscape: Development of a fen-bog complex in the Sporadic Discontinuous Permafrost zone of northern Alberta, Canada. *Boreas*, *40*, 714-726. <https://doi.org/10.1111/j.1502-3885.2011.00210.x>
- Bekryaev, R. V., Polyakov, I. V., & Alexeev, V. A. (2010). Role of polar amplification in long-term surface air temperature variations and modern Arctic warming. *Journal of Climate*, *23*, 3888-3906. <https://doi.org/10.1175/2010JCLI3297.1>
- Blaauw, M. (2010). Methods and code for 'classical' age-modelling of radiocarbon sequences. *Quaternary Geochronology*, *5*, 512-518. <https://doi.org/10.1016/j.quageo.2010.01.002>
- Blaauw, M., & Christen, J. A. (2011). Flexible paleoclimate age-depth models using an autoregressive gamma process. *Bayesian Analysis*, *6*, 457-474.
<https://doi.org/10.1214/11-BA618>
- Blaauw, M., Christen, J. A., Bennett, K. D., & Reimer, P. J. (2018). Double the dates and go for Bayes – Impacts of model choice, dating density and quality on chronologies. *Quaternary Science Reviews*, *188*, 58-66. <https://doi.org/10.1016/j.quascirev.2018.03.032>
- Botch, M. S., Kobak, K. I., Vinson, T. S., & Kolchugina, T. P. (1995). Carbon pools and accumulation in peatlands of the former Soviet Union. *Global Biogeochemical Cycles*, *9*, 37-46. <https://doi.org/10.1029/94GB03156>
- Bragazza, L., Buttler, A., Habermacher, J., Brancaloni, L., Gerdol, R., Fritze, H., et al. (2012). High nitrogen deposition alters the decomposition of bog plant litter and reduces carbon accumulation. *Global Change Biology*, *18*, 1163-1172.
<https://doi.org/10.1111/j.1365-2486.2011.02585.x>
- Brown, J., OJ Ferrians, Jr., Heginbottom, J. A., & Melnikov, E. S. (1998). revised February 2001.

- Circum-arctic map of permafrost and ground ice conditions. Boulder, CO: National Snow and Ice Data Center. Digital media.
- Bulygina, O. N., & Razuvaev, V. N. (2012). Daily temperature and precipitation data for 518 Russian meteorological stations, Carbon Dioxide Information Analysis Center, Oak Ridge National Laboratory, U.S. Department of Energy, Oak Ridge, Tennessee.
<http://doi.org/10.3334/CDIAC/cli.100>
- Camill, P., Lynch, J. A., Clark, J. S., Adams, J. B., & Jordan, B. (2001). Changes in biomass, aboveground net primary production, and peat accumulation following permafrost thaw in the boreal peatlands of Manitoba, Canada. *Ecosystems*, 4, 461-478.
<https://doi.org/10.1007/s10021-001-0022-3>
- Chadburn, S. E., Burke, E. J., Cox, P. M., Friedlingstein, P., Hugelius, G., & Westermann, S. (2017). An observation-based constraint on permafrost loss as a function of global warming. *Nature Climate Change*, 7, 340-344. <https://doi.org/10.1038/nclimate3262>
- Charman, D. J., Amesbury, M. J., Hinchliffe, W., Hughes, P. D. M., Mallon, G., Blake, W. H., et al. (2015). Drivers of Holocene peatland carbon accumulation across a climate gradient in northeastern North America. *Quaternary Science Reviews*, 121, 110-119.
<https://doi.org/10.1016/j.quascirev.2015.05.012>
- Charman, D. J., Beilman, D. W., Blaauw, M., Booth, R. K., Brewer, S., Chambers, F. M., et al. (2013). Climate-related changes in peatland carbon accumulation during the last millennium. *Biogeosciences*, 10, 929-944. <https://doi.org/10.5194/bg-10-929-2013>
- Chaudhary, N., Miller, P. A., & Smith, B. (2017). Modelling past, present and future peatland carbon accumulation across the pan-Arctic region. *Biogeosciences*, 14, 4023-4044.
<https://doi.org/10.5194/bg-14-4023-2017>
- Clymo, R. S. (1984). The limits to peat bog growth. *Philosophical Transactions of the Royal Society of London. Series B, Biological Sciences*, 303, 605-654.
- Estop-Aragonés, C., Cooper, M. D. A., Fisher, J. P., Thierry, A., Garnett, M. H., Charman, D. J., et al. (2018). Limited release of previously-frozen C and increased new peat formation after thaw in permafrost peatlands. *Soil Biology and Biochemistry*, 118, 115-129.
<https://doi.org/10.1016/j.soilbio.2017.12.010>
- Faucherre, S., Jorgensen, C. J., Blok, D., Weiss, N., Siewert, M. B., Bang-Andreasen, T., Hugelius, G., Kuhry, P., & Elberling, B. (2018). Short and long-term controls on active layer and permafrost carbon turnover across the Arctic. *Journal of Geophysical Research: Biogeosciences*, 123, 372-390. <https://doi.org/10.1002/2017JG004069>
- Field, C. B., Randerson, J. T., & Malmström, C. M. (1995). Global net primary production: combining ecology and remote sensing. *Remote Sensing of Environment*, 51: 74-88.
[https://doi.org/10.1016/0034-4257\(94\)00066-V](https://doi.org/10.1016/0034-4257(94)00066-V)
- Frolking, S., Roulet, N. T., Moore, T. R., Richard, P. J. H., Lavoie, M., & Muller, S. D. (2001). Modeling northern peatland decomposition and peat accumulation. *Ecosystems*, 4, 479-498. <https://doi.org/10.1007/s10021-001-0105-1>

- Gałka, M., Szal, M., Watson, E. J., Gallego-Sala, A. V., Amesbury, M. J., Charman, D. J., et al. (2017). Vegetation succession, carbon accumulation and hydrological change in subarctic peatlands, Abisko, northern Sweden. *Permafrost and Periglacial Processes*, 28, 589-604. <https://doi.org/10.1002/ppp.1945>
- Gallego-Sala, A. V., & Prentice, I. C. (2013). Blanket peat biome endangered by climate change. *Nature Climate Change*, 3, 152-155. <https://doi.org/10.1038/nclimate1672>
- Gao, Y., & Couwenberg, J. (2015). Carbon accumulation in a permafrost polygon peatland: steady long-term rates in spite of shifts between dry and wet conditions. *Global Change Biology*, 21, 803-815. <https://doi.org/10.1111/gcb.12742>
- Garneau, M., van Bellen, S., Magnan, G., Beaulieu-Audy, V., Lamarre, A., & Asnong, H. (2014). Holocene carbon dynamics of boreal and subarctic peatlands from Quebec, Canada. *The Holocene*, 24, 1043-1053. <https://doi.org/10.1177/0959683614538076>
- Hartmann, D. L., Klein Tank, A. M. G., Rusticucci, M., Alexander, L. V., Brönnimann, S., Charabi, Y., et al. (2013). Observations: Atmosphere and Surface. In T. F. Stocker, D. Qin, G. K. Plattner, M. Tignor, S. K. Allen, J. Boschung, et al. (Eds.), *Climate Change 2013: The Physical Science Basis*. Contribution of Working Group I to the Fifth Assessment Report of the Intergovernmental Panel on Climate Change. Cambridge University Press, Cambridge, United Kingdom and New York, NY, USA.
- Helama, S., Meriläinen, J., & Tuomenvirta, H. (2009). Multicentennial megadrought in northern Europe coincided with a global El Niño-Southern Oscillation drought pattern during the Medieval Climate Anomaly. *Geology*, 37, 175-178. <https://doi.org/10.1130/G25329A.1>
- Hodgkins, S. B., Tfaily, M. M., McCalley, C. K., Logan, T. A., Crill, P. M., Saleska, S. R., et al. (2014). Changes in peat chemistry associated with permafrost thaw increase greenhouse gas production. *Proceedings of the National Academy of Sciences of the United States of America*, 111, 5819-5824. <https://doi.org/10.1073/pnas.1314641111>
- Hua, Q., Barbetti, M., & Rakowski, A. Z. (2013). Atmospheric radiocarbon for the period 1950–2010. *Radiocarbon*, 55, 2059-2072. https://doi.org/10.2458/azu_js_rc.v55i2.16177
- Hugelius, G., Routh, J., Kuhry, P., & Crill, P. (2012). Mapping the degree of decomposition and thaw remobilization potential of soil organic matter in discontinuous permafrost terrain. *Journal of Geophysical Research*, 117, G02030. <http://doi.org/10.1029/2011JG001873>
- Hunt, S., Yu, Z. C., & Jones, M. (2013). Lateglacial and Holocene climate, disturbance and permafrost peatland dynamics on the Seward Peninsula, western Alaska. *Quaternary Science Reviews*, 63, 42-58. <https://doi.org/10.1016/j.quascirev.2012.11.019>
- Jones, B. M., Baughman, C. A., Romanovsky, V. E., Parsekian, A. D., Babcock, E. L., Stephani, E., et al. (2016). Presence of rapidly degrading permafrost plateaus in south-central Alaska. *The Cryosphere*, 10, 2673-2692. <https://doi.org/10.5194/tc-10-2673-2016>
- Jones, M. C., Harden, J., O'Donnell, J., Manies, K., Jorgenson, T., Treat, C., & Ewing, S. (2017). Rapid carbon loss and slow recovery following permafrost thaw in boreal peatlands. *Global Change Biology*, 23, 1109-1127. <https://doi.org/10.1111/gcb.13403>
- Kelly, T. J., Lawson, I. T., Roucoux, K. H., Baker, T. R., Jones, T. D., & Sanderson, N. K. (2017). The vegetation history of an Amazonian domed peatland. *Palaeogeography*

- Palaeoclimatology Palaeoecology*, 468, 129-141.
<https://doi.org/10.1016/j.palaeo.2016.11.039>
- Klein, E. S., Booth, R. K., Yu, Z., Mark, B. G., & Stansell, N. D. (2013b). Hydrology-mediated differential response of carbon accumulation to late Holocene climate change at two peatlands in Southcentral Alaska. *Quaternary Science Reviews*, 64, 61-75.
<https://doi.org/10.1016/j.quascirev.2012.12.013>
- Klein, E. S., Yu, Z. C., & Booth, R. K. (2013a). Recent increase in peatland carbon accumulation in a thermokarst lake basin in southwestern Alaska. *Palaeogeography Palaeoclimatology Palaeoecology*, 392, 186-195. <https://doi.org/10.1016/j.palaeo.2013.09.009>
- Kokfelt, U., Rosen, P., Schoning, K., Christensen, T. R., Förster, J., Karlsson, J., et al. (2009). Ecosystem responses to increased precipitation and permafrost decay in subarctic Sweden inferred from peat and lake sediments. *Global Change Biology*, 15, 1652-1663.
<https://doi.org/10.1111/j.1365-2486.2009.01880.x>
- Kremenetski, K. V., Boettger, T., MacDonald, G. M., Vaschalova, T., Sulerzhitsky, L., & Hiller, A. (2004). Medieval climate warming and aridity as indicated by multiproxy evidence from the Kola Peninsula Russia. *Palaeogeography Palaeoclimatology Palaeoecology*, 209, 113-125. <https://doi.org/10.1016/j.palaeo.2004.02.018>
- Lamarre, A., Garneau, M., & Asnong, H. (2012). Holocene paleohydrological reconstruction and carbon accumulation of a permafrost peatland using testate amoeba and macrofossil analyses, Kuujuarapik, subarctic Quebec, Canada. *Review of Palaeobotany and Palynology*, 186, 131-141. <https://doi.org/10.1016/j.revpalbo.2012.04.009>
- Linderholm, H. W., Nicolle, M., Francus, P., Gajewski, K., Helama, S., Korhola, A., et al. (2018). Arctic hydroclimate variability during the last 2000 years: current understanding and research challenges. *Climate of the Past*, 14, 473-514.
<https://doi.org/10.5194/cp-14-473-2018>
- Loisel, J., & Garneau, M. (2010). Late Holocene paleoecohydrology and carbon accumulation estimates from two boreal peat bogs in eastern Canada: Potential and limits of multiproxy archives. *Palaeogeography Palaeoclimatology Palaeoecology*, 291, 493-533.
<https://doi.org/10.1016/j.palaeo.2010.03.020>
- Loisel, J., & Yu, Z. C. (2013a). Recent acceleration of carbon accumulation in a boreal peatland, south central Alaska. *Journal of Geophysical Research: Biogeosciences*, 118, 41-53.
<https://doi.org/10.1029/2012JG001978>
- Loisel, J., & Yu, Z. C. (2013b). Surface vegetation patterning controls carbon accumulation in peatlands. *Geophysical Research Letters*, 40, 5508-5513.
<https://doi.org/10.1002/grl.50744>
- Loisel, J., Yu, Z. C., Beilman, D. W., Camill, P., Alm, J., Amesbury, M. J., et al. (2014). A database and synthesis of northern peatland soil properties and Holocene carbon and nitrogen accumulation. *The Holocene*, 24, 1028-1042.
<https://doi.org/10.1177/0959683614538073>

- Mann, M. E. (2002). Medieval Climatic Optimum. In M. C. MacCracken & J. S. Perry (Eds.), *Encyclopedia of Global Environmental Change* (pp. 514-516). John Wiley, Chichester, UK.
- McLaughlin, J., & Webster, K. (2014). Effects of climate change on peatlands in the far north of Ontario, Canada: a synthesis. *Arctic, Antarctic, and Alpine Research*, *46*, 88-102. <https://doi.org/10.1657/1938-4246-46.1.84>
- Mathijssen, P. J. H., Väiliranta, M., Korrensalo, A., Alekseychik, P., Vesala, T., Rinne, J., & Tuittila, E.-S. (2016). Reconstruction of Holocene carbon dynamics in a large boreal peatland complex, southern Finland. *Quaternary Science Reviews*, *142*, 1-15. <https://doi.org/10.1016/j.quascirev.2016.04.013>
- Mathijssen, P. J. H., Kähkölä, N., Tuovinen, J. P., Lohila, A., Minkkinen, K., Laurila, T., & Väiliranta, M. (2017). Lateral expansion and carbon exchange of a boreal peatland in Finland resulting in 7000 years of positive radiative forcing. *Journal of Geophysical Research: Biogeosciences*, *122*, 562-577. <https://doi.org/10.1002/2016JG003749>
- Mikkonen, S., Laine, M., Makela, H. M., Gregow, H., Tuomenvirta, H., Lahtinen, M., & Laaksonen, A. (2015). Trends in the average temperature in Finland, 1847-2013. *Stochastic Environmental Research and Risk Assessment*, *29*, 1521-1529. <https://doi.org/10.1007/s00477-014-0992-2>
- Nichols, J. E., Peteet, D. M., Moy, C. M., Castaneda, I. S., McGeachy, A., & Peres, M. (2014). Impacts of climate and vegetation change on carbon accumulation in a south-central Alaskan peatland assessed with novel organic geochemical techniques. *The Holocene*, *24*, 1146-1155. <https://doi.org/10.1177/0959683614540729>
- Oberman, N. G. (2008). Contemporary Permafrost Degradation of Northern European Russia. In D. L. Kane, & K. M. Hinkel (Eds.), *Proceedings of the Ninth International Conference on Permafrost* (pp. 1305-1310), Fairbanks, Alaska.
- O'Donnell, J. A., Jorgenson, M. T., Harden, J. W., McGuire, A. D., Kanevskiy, M. Z., & Wickland, K. P. (2012). The effect of permafrost thaw on soil hydrologic, thermal, and carbon dynamics in an Alaskan peatland. *Ecosystems*, *15*, 213-229. <https://doi.org/10.1007/s10021-011-9504-0>
- Oksanen, P. O. (2006) Holocene development of the Vaisjeaggi palsa mire, Finnish Lapland. *Boreas*, *35*, 81-95. <https://doi.org/10.1080/03009480500359103>
- Oksanen, P. O., Kuhry, P., & Alekseeva, R. N. (2003). Holocene development and permafrost history of the Usinsk mire, northeast European Russia. *Géographie physique et Quaternaire*, *57*, 169-187. <https://doi.org/10.7202/011312ar>
- Pelletier, N., Talbot, J., Olefeldt, D., Turetsky, M., Blodau, C., Sonnentag, O., & Quinton, W. L. (2017). Influence of Holocene permafrost aggradation and thaw on the paleoecology and carbon storage of a peatland complex in northwestern Canada. *The Holocene*, *27*, 1391-1405. <https://doi.org/10.1177/0959683617693899>
- Pirinen, P., Simola, H., Aalto, J., Kaukoranta, J. P., Karlsson, P., & Ruuhela, R. (2012). Tilastoja Suomen ilmastosta 1981–2010 (Climatological statistics of Finland 1981–2010). Finnish

Meteorological Institute Reports, 1.

- Reimer, P. J., Bard, E., Bayliss, A., Beck, J. W., Blackwell, P. G., Ramsey, C. B., et al. (2013). IntCal13 and Marine13 radiocarbon age calibration curves, 0-50, 000 years cal BP. *Radiocarbon*, 55, 1869-1887. https://doi.org/10.2458/azu_js_rc.55.16947
- R Core Team. (2014). R: A language and environment for statistical computing. R Foundation for Statistical Computing, Vienna, Austria.
- Repo, M. E., Susiluoto, S., Lind, S. E., Jokinen, S., Elsakov, V., Biasi, C., et al. (2009). Large N₂O emissions from cryoturbated peat soil in tundra. *Nature Geoscience*, 2, 189-192. <https://doi.org/10.1038/ngeo434>
- Robinson, S. D. (2006). Carbon accumulation in peatlands, southwestern Northwest Territories, Canada. *Canadian Journal of Soil Science*, 86, 305-319. <https://doi.org/10.4141/S05-086>
- Romanovsky, V. E., Drozdov, D. S., Oberman, N. G., Malkova, G. V., Kholodov, A. L., Marchenko, S. S., et al. (2010). Thermal state of permafrost in Russia. *Permafrost and Periglacial Processes*, 21, 136-155. <https://doi.org/10.1002/ppp.683>
- Ronkainen, T., Väiliranta, M., McClymont, E., Biasi, C., Salonen, S., Fontana, S., & Tuittila, E.-S. (2015). A combined biogeochemical and palaeobotanical approach to study permafrost environments and past dynamics. *Journal of Quaternary Science*, 30, 189-200. <https://doi.org/10.1002/jqs.2763>
- Routh, J., Hugelius, G., Kuhry, P., Filley, T., Tillman, P. K., Becher, M., & Crill, P. (2014). Multi-proxy study of soil organic matter dynamics in permafrost peat deposits reveal vulnerability to climate change in the European Russian Arctic. *Chemical Geology*, 368, 104-117. <https://doi.org/10.1016/j.chemgeo.2013.12.022>
- Sannel, A. B. K., & Kuhry, P. (2009). Holocene peat growth and decay dynamics in sub-arctic peat plateaus, west-central Canada. *Boreas*, 38, 13-24. <https://doi.org/10.1111/j.1502-3885.2008.00048.x>
- Sannel, A. B. K., Hempel, L., Kessler, A., & Preskienis, V. (2017). Holocene development and permafrost history in sub-arctic peatlands in Tavvavuoma, northern Sweden. *Boreas*, 47, 454-468. <https://doi.org/10.1111/bor.12276>
- Saugier, B., Roy, J., & Mooney, H. A. (2001). Estimations of global terrestrial productivity: converging toward a single number?. In R. Jacques, S. Bernard, & A. M. Harold (Eds.), *Terrestrial Global Productivity* (pp. 543-557), Elsevier.
- Schuur, E. A., Vogel, J. G., Crummer, K. G., Lee, H., Sickman, J. O., & Osterkamp, T. E. (2009). The effect of permafrost thaw on old carbon release and net carbon exchange from tundra. *Nature*, 459, 556-559. <https://doi.org/10.1038/nature08031>
- Schuur, E. A., McGuire, A. D., Schädel, C., Grosse, G., Harden, J. W., Hayes, D. J., et al. (2015). Climate change and the permafrost carbon feedback. *Nature*, 520, 171-179. <https://doi.org/10.1038/nature14338>
- Seppälä, M. (2006). Palsa mires in Finland. *The Finnish Environment*, 23, 155-162.
- Swindles, G. T., Morris, P. J., Mullan, D., Watson, E. J., Turner, T. E., Roland, T. P., et al.

- (2015). The long-term fate of permafrost peatlands under rapid climate warming. *Scientific Reports*, 5. <http://doi.org/10.1038/srep17951>
- Tolonen, K., & Turunen, J. (1996). Accumulation rates of carbon in mires in Finland and implications for climate change. *The Holocene*, 6, 171-178.
<https://doi.org/10.1177/095968369600600204>
- Treat, C. C., Jones, M. C., Camill, P., Gallego-Sala, A., Garneau, M., Harden, J. W., et al. (2016). Effects of permafrost aggradation on peat properties as determined from a pan-Arctic synthesis of plant macrofossils. *Journal of Geophysical Research: Biogeosciences*, 121, 78-94. <https://doi.org/10.1002/2015JG003061>
- Treat, C. C., Wollheim, W. M., Varner, R. K., Grandy, A. S., Talbot, J., & Frohling, S. (2014). Temperature and peat type control CO₂ and CH₄ production in Alaskan permafrost peats. *Global Change Biology*, 20, 2674-2686. <https://doi.org/10.1111/gcb.12572>
- Turunen, J. (2003). Past and present carbon accumulation in undisturbed boreal and subarctic mires: A review. *Suoseura*, 54, 15-28.
- van Bellen, S., Dallaire, P.-L., Garneau, M., & Bergeron, Y. (2011). Quantifying spatial and temporal Holocene carbon accumulation in ombrotrophic peatlands of the Eastmain region, Quebec, Canada. *Global Biogeochemical Cycles*, 25, GB2016.
<https://doi.org/10.1029/2010GB003877>
- Väliranta, M., Blundell, A., Charman, D. J., Karofeld, E., Korhola, A., Sillasoo, U., & Tuittila, E.-S. (2012). Reconstructing peatland water tables using transfer functions for plant macrofossils and testate amoebae: A methodological comparison. *Quaternary International*, 268, 34-43. <https://doi.org/10.1016/j.quaint.2011.05.024>
- Väliranta, M., Korhola, A., Seppä, H., Tuittila, E.-S., Sarmaja-Korjonen, K., Laine, J., & Alm, J. (2007). High-resolution reconstruction of wetness dynamics in a southern boreal raised bog, Finland, during the late Holocene: a quantitative approach. *The Holocene*, 17, 1093-1107. <https://doi.org/10.1177/0959683607082550>
- Wang, M., Yang, G., Gao, Y., Chen, H., Wu, N., Peng, C., et al. (2015). Higher recent peat C accumulation than that during the Holocene on the Zoige Plateau. *Quaternary Science Reviews*, 114, 116-125. <https://doi.org/10.1016/j.quascirev.2015.01.025>
- Wilson, R., Anchukaitis, K., Briffa, K. R., Büntgen, U., Cook, E., D'Arrigo, R., et al. (2016). Last millennium northern hemisphere summer temperatures from tree rings: Part I: The long term context. *Quaternary Science Review*, 134, 1-18.
<https://doi.org/10.1016/j.quascirev.2015.12.005>
- Wilson, R. M., Fitzhugh, L., Whiting, G. J., Frohling, S., Harrison, M. D., Dimova, N., et al. (2017). Greenhouse gas balance over thaw-freeze cycles in discontinuous zone permafrost. *Journal of Geophysical Research: Biogeosciences*, 122, 387-404.
<https://doi.org/10.1002/2016JG003600>
- Xing, W., Bao, K., Gallego-Sala, A. V., Charman, D. J., Zhang, Z., Gao, C., et al. (2015). Climate controls on carbon accumulation in peatlands of Northeast China. *Quaternary Science Reviews*, 115, 78-88. <https://doi.org/10.1016/j.quascirev.2015.03.005>

- Yu, Z. C., Loisel, J., Brosseau, D. P., Beilman, D. W., & Hunt, S. J. (2010). Global peatland dynamics since the Last Glacial Maximum. *Geophysical Research Letters*, *37*, L13402. <http://doi.org/10.1029/2010gl043584>
- Yu, Z. C. (2011). Holocene carbon flux histories of the world's peatlands: Global carbon-cycle implications. *The Holocene*, *21*, 761-774. <https://doi.org/10.1177/0959683610386982>
- Yu, Z. C., Campbell, I. D., Vitt, D. H., & Apps, M. J. (2001). Modelling long-term peatland dynamics. I. Concepts, review, and proposed design. *Ecological Modelling*, *145*, 197-210. [https://doi.org/10.1016/S0304-3800\(01\)00391-X](https://doi.org/10.1016/S0304-3800(01)00391-X)
- Yu, Z. C., Beilman, D. W., & Jones, M. C. (2009). Sensitivity of Northern Peatland Carbon Dynamics to Holocene Climate Change. In A. J. Baird, L. R. Belyea, X. Comas, A.S. Reeve, & L. D. Slater (Eds.), *Carbon Cycling in Northern Peatlands*. American Geophysical Union, Washington, D.C.. <http://doi.org/10.1029/2008GM000822>
- Zhang, H., Amesbury, M. J., Ronkainen, T., Charman, D. J., Gallego-Sala, A. V., & Väliranta, M. (2017). Testate amoeba as palaeohydrological indicators in the permafrost peatlands of north-east European Russia and Finnish Lapland. *Journal of Quaternary Science*, *32*, 976-988. <https://doi.org/10.1002/jqs.2970>
- Zhang, H., Piilo, S., Amesbury, M. J., Charman, D. J., Gallego-Sala, A. V., & Väliranta, M. V. (2018). The role of climate in regulating Arctic permafrost peatland hydrological and vegetation change over the last millennium. *Quaternary Science Reviews*, *82*, 121-130. <https://doi.org/10.1016/j.quascirev.2018.01.003>
- Zhang, L., Guo, H. D., Ji, L., Lei, L. P., Wang, C. Z., Yan, D. M., et al. (2013). Vegetation greenness trend (2000 to 2009) and the climate controls in the Qinghai-Tibetan Plateau. *Journal of Applied Remote Sensing*, *7*, 073572. <https://doi.org/10.1117/1.JRS.7.073572>

Supporting Information for

Inconsistent response of Arctic permafrost peatland carbon accumulation to warm climate phases

H. Zhang^{1,2}, A. V. Gallego-Sala³, M. J. Amesbury^{1,3}, D. J. Charman³, S. R. Piilo^{1,2}, and M. M. Väiliranta^{1,2}

¹ECRU, Ecosystems and Environment Research Programme, Faculty of Biological and Environmental Sciences, University of Helsinki, P.O. Box 65, 00014, Finland

²Helsinki Institute of Sustainability Science (HELSUS), Finland.

³Geography, College of Life and Environmental Sciences, University of Exeter, UK.

Contents of this file

Figures S1 to S2

Tables S1 to S4

Introduction

This supporting information provides the age-depth models of studied 14 peat cores (Fig. S1) and non-autogenic carbon accumulation patterns for 14 peat cores (Fig. S2). Table S1 shows radiocarbon dating and peat property details. Table S2-S3 show the derived parameters and results from the used modeling approaches. Table S4 shows the results of multiple linear regression analysis of apparent carbon accumulation and environmental variables.

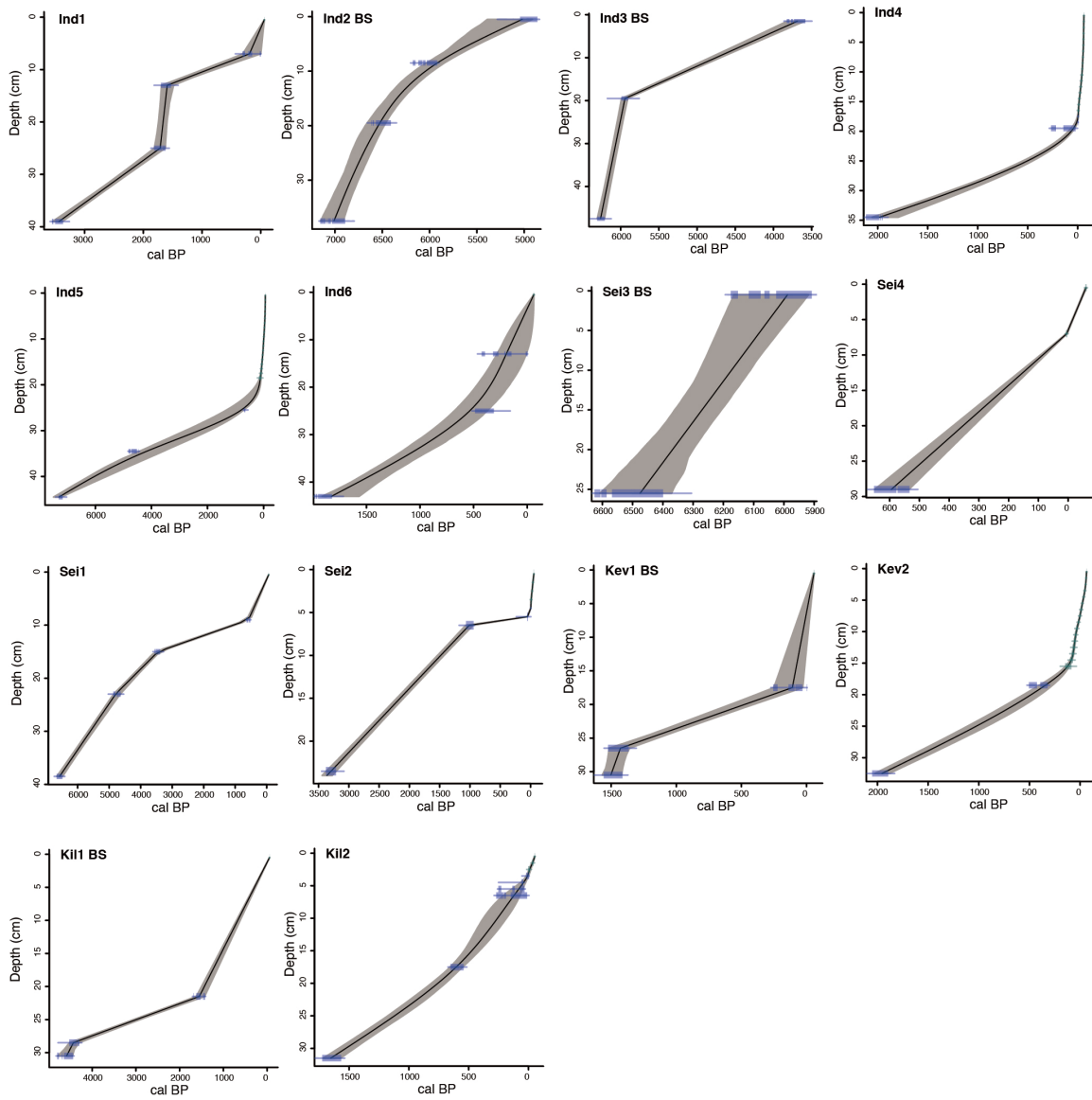


Fig. S1. Age-depth models of studied peat cores from four permafrost peatlands. Post-bomb dates are shown in green and pre-bomb dates are shown in blue.

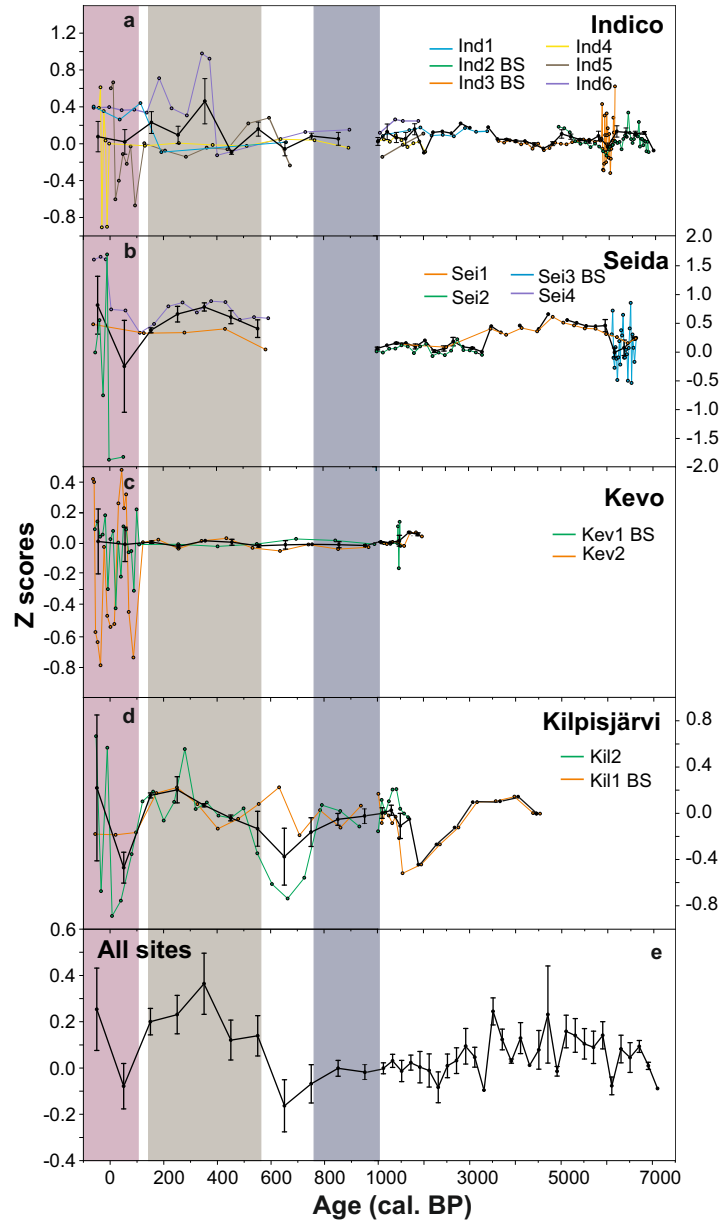


Fig. S2. (a-d) Non-autogenic carbon accumulation z scores for four permafrost peatlands with error bars representing standard errors of the means. Up to 1000 yrs BP, calculations are for each 100-yr bin, for later periods, calculations are for each 200-yr bin. (e) Combined data for all sites are shown. Samples that may be influenced by uncertainty of ^{14}C dating were removed (see text for details). Climate phases are indicated using purple (Medieval Climate Anomaly), grey (Little Ice Age) and red (recent warming) shadings.

Core	Dated depth (cm)	Age (BP)	cal. BP	PAR range	BD (g cm ⁻³)	LOI (%)	C (%)	N (%)	C/N ratio
Ind1	6-8	220 ± 30	235	0.04-1.00	0.11 ± 0.02	78.14 ± 7.67	-	-	-
	12-14	1686 ± 40	1615						
	24-26	1785 ± 30	1700						
	38-40	3216 ± 36	3420						
Ind2 BS	0-1	4385 ± 35	4950	0.08-0.43	0.08 ± 0.02	-	49.95 ± 1.59	0.83 ± 0.18	62.42 ± 11.05
	8-9	5240 ± 35	6035						
	19-20	5708 ± 30	6490						
	37-38	6109 ± 31	7040						
Ind3 BS	1-2	3425 ± 35	3660	0.08-0.88	0.07 ± 0.03	-	50.68 ± 1.33	0.41 ± 0.18	148.61 ± 65.44
	19-20	5182 ± 28	5950						
	47-48	5466 ± 31	6260						
Ind4	19-20	109 ± 22	125	0.07-2.00	0.09 ± 0.04	-	48.22 ± 3.24	1.25 ± 0.43	35.25 ± 8.11
	34-35	2066 ± 25	2050						
Ind5	25-26	726 ± 24	675	0.02-1.23	0.10 ± 0.06	-	44.92 ± 4.18	1.00 ± 0.51	36.26 ± 6.91
	34-35	4105 ± 35	4700						
	44-45	6308 ± 33	7230						
Ind6	12-14	240 ± 30	230	0.06-0.70	0.07 ± 0.02	79.22 ± 5.54	-	-	-
	24-26	345 ± 35	400						
	42-44	1941 ± 35	1885						
Sei1	8-10	560 ± 30	580	0.02-0.13	0.17 ± 0.08	71.04 ± 18.9	-	-	-
	14-16	3230 ± 35	3495						
	22-24	4245 ± 40	4780						
	38-39	5775 ± 38	6575						
Sei2	6-7	1105 ± 30	1010	0.01-1.43	0.20 ± 0.05	-	50.26 ± 1.62	2.26 ± 0.61	24.48 ± 8.78
	7-8	1050 ± 30	* 965						
	23-24	3085 ± 30	3295						
Sei3 BS	0-1	5220 ± 40	5970	0.48	0.07 ± 0.01	-	51.79 ± 0.80	2.27 ± 0.22	23.17 ± 2.27
	25-26	5690 ± 40	6485						
Sei4	6-8	100.51 ± 0.34 (pMC)	-5	0.04-0.1	0.07 ± 0.01	93.71 ± 5.70	-	-	-
	28-30	580 ± 37	580						
Kev1 BS	0-1	105.92 ± 0.34 (pMC)	-57	0.07-1.03	0.11 ± 0.03	-	52.67 ± 0.79	1.69 ± 0.11	31.23 ± 2.08
	17-18	50 ± 30	140						
	26-27	1540 ± 30	1445						
	30-31	1610 ± 30	1485						
Kev2	18-19	380 ± 30	410	0.08-2.53	0.14 ± 0.04	-	51.62 ± 2.07	1.83 ± 0.38	29.35 ± 5.83
	32-33	2020 ± 30	1975						
Kill1 BS	0-1	106.57 ± 0.34 (pMC)	-56	0.02-0.13	0.15 ± 0.02	-	51.84 ± 2.40	2.05 ± 0.15	25.27 ± 2.00
	21-22	1650 ± 30	1570						
	28-29	3965 ± 35	4450						
	30-31	4065 ± 35	4540						
	39-40	3575 ± 30	* 3900						
Kil2	17-18	600 ± 30	585	0.12-0.57	0.13 ± 0.02	-	47.68 ± 6.17	1.77 ± 0.26	27.86 ± 6.46
	20-21	495 ± 30	* 525						
	31-32	1750 ± 30	1645						
All cores					0.13 ± 0.06	79.67 ± 13.86	50.23 ± 4.37	1.49 ± 0.70	51.94 ± 50.71

PAR: peat accumulation rate (mm yr⁻¹); BD: bulk density; LOI: loss on ignition. The values of BD, LOI, C and N content (%) are present as mean ± standard deviation. pMC: percentage modern carbon. *Ages are removed from age-depth modeling.

Table S1. Radiocarbon dating details and peat properties of peat cores in this study.

	Dec _{part} peat			Dec _{full} peat				Dec _{part} peat			Dec _{full} peat		
	<i>p</i>	<i>α</i>	adj.R ²	<i>p</i>	<i>α</i>	adj.R ²		<i>p</i>	<i>α</i>	adj.R ²	<i>p</i>	<i>α</i>	adj.R ²
Ind1	19.44 ± 4.78	35.65	0.9847	<i>40.10 ± 1.15</i>	<i>2.00</i>	<i>0.9883</i>	Sei4	34.07 ± 0	49.98	0.9999	12.60 ± 0.18	3.00	0.9926
				4.46 ± 0.50	0.24	0.9879	Kev1 BS	87.30 ± 1.43	8.70	0.9999	10.00 ± 0.24	2.75	0.9853
Ind4	187.90 ± 14.27	117.70	0.9934	12.90 ± 0.12	2.48	0.9997					<i>79.30 ± 2.58</i>	<i>5.40</i>	<i>0.9885</i>
Ind5	68.29 ± 2.66	50.29	0.9982	17.94 ± 1.32	9.57	0.9829	Kev2	154.70 ± 8.36	53.58	0.9910	15.50 ± 0.25	0.18	0.9992
Ind6	12.50 ± 0.21	4.11	0.9917	4.32 ± 0.58	1.09	0.9825	Kil1 BS	22.3 ± 0.75	12.1	0.9909	28.40 ± 1.04	8.43	0.9841
Sei1	2.79 ± 0	5.55	0.9999	5.19 ± 0	0.29	0.8828					<i>22.20 ± 0.63</i>	<i>2.46</i>	<i>0.9999</i>
Sei2	98.97 ± 9.84	114.80	0.9846	17.37 ± 0.14	0.24	0.9997	Kil2	62.69 ± 4.21	63.46	0.9954	29.60 ± 0.46	4.18	0.9984

Values in italic represent the sections that may be impacted by the uncertainty of dating and removed from further analysis.

Table S2. Results of the exponential decay modeling of all studied peat cores, with partially decomposed (Dec_{part}) and fully decomposed (Dec_{full}) peat sections processed separately. *p*: peat addition rate (g m⁻² yr⁻¹), *α*: peat decay coefficient (*10⁻⁴ yr⁻¹).

	Remaining C mass (g m ⁻² yr ⁻¹)			NCU (g m ⁻² yr ⁻¹)		Remaining C mass (g m ⁻² yr ⁻¹)			NCU (g m ⁻² yr ⁻¹)
	initial input	after 100 yrs	after 300 yrs			initial input	after 100 yrs	after 300 yrs	
Ind1	9.72	8.82	4.70	4.04	Sei4	17.35	11.36	6.82	12.6
Ind4	93.95	43.16	20.73	6.56	Kev1 BS	43.65	40.16	34.61	5.63
Ind5	34.15	22.72	13.61	9.21	Kev2	77.35	50.36	29.67	8.00
Ind6	6.25	6.00	5.56	7.11	Kil1 BS	11.15	9.95	8.18	7.83
Sei1	1.40	1.32	1.20	4.94	Kil2	31.35	19.18	10.79	13.77
Sei2	49.49	23.04	11.14	8.70					

Table S3. Comparisons between the expected remaining C mass of present peat after 100, 300 years decomposition and the net peat C uptake (NCU) of past few millennia.

	β -Coefficients (SE)	Standardized β	95% CI	<i>p</i> -value
Intercept	57.24 (18.74)	-	19.82 to 94.66	0.003
T _{sum}	22.53 (6.94)	0.32	8.68 to 36.39	0.002
WTD	6.28 (2.59)	0.24	1.11 to 11.46	0.018
UOM	-0.40 (0.16)	-0.26	-0.72 to -0.07	0.017
N%	-13.99 (8.51)	-0.24	-30.97 to 2.99	0.11
C/N ratio	-0.16 (0.23)	-0.09	-0.62 to 0.30	0.50
Herbaceous	-0.01 (0.14)	-0.01	-0.29 to 0.28	0.97
Ligneous	0.09 (0.09)	0.11	-0.09 to 0.27	0.30

T_{sum}: summer temperature; WTD: water-table depth; UOM: unidentifiable organic matter; N%: nitrogen content; C/N: carbon/nitrogen; CI: confidence interval.

* adj. R² = 0.42, *p* < 0.001.

Table S4. Multiple linear regression modeling* of relationship between apparent carbon accumulation rates and environmental variables for all sites combined dataset.